Optofluidic Intracavity Spectroscopy for Spatially, Temperature, and Wavelength Dependent Refractometry

MS Final Exam

Joel Kindt

Advisor: Prof. Kevin L. Lear

Committee members:
Prof. Kristen Buchanan
Prof. Branislav Notaros

Department of Electrical and Computer Engineering
Colorado State University

July 3rd, 2012

Outline

- Motivation and background
- Computer modeling
- Experimental materials and methods
- Experimental results
- Summary

Outline

- Motivation and background
  - Our optofluidic device
  - Lab refractometers
  - Microfluidic FP refractometers
- Computer modeling
- Experimental materials and methods
- Experimental results
- Summary

Our optofluidic device

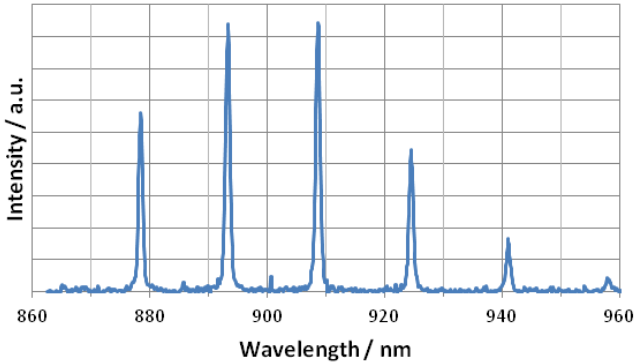

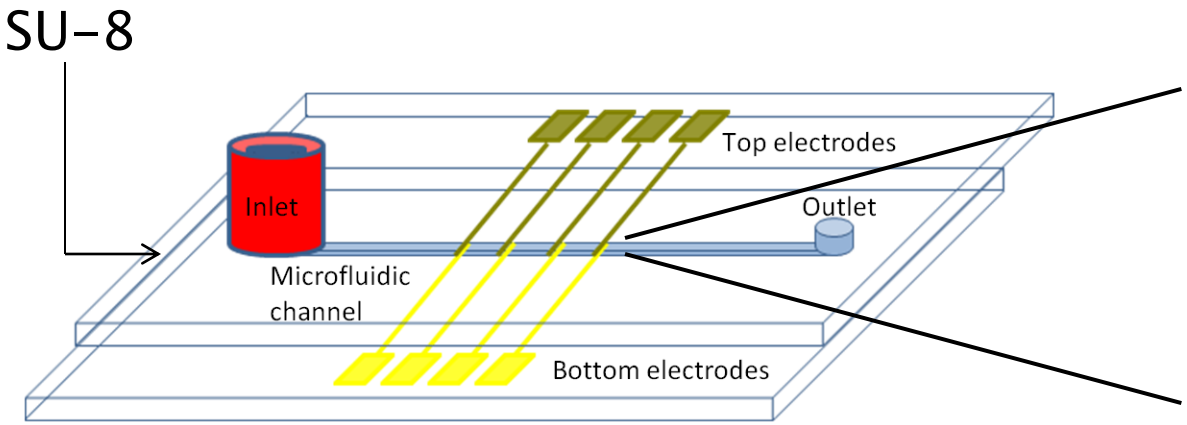

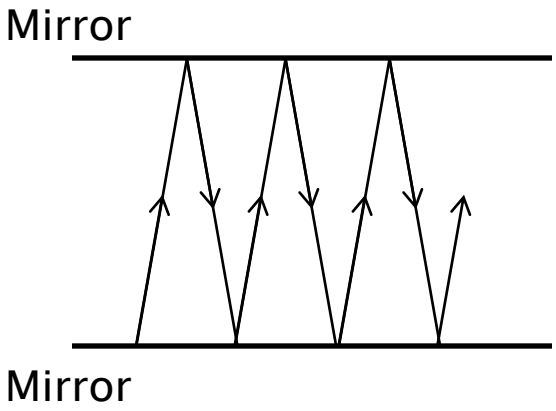

IR LED

➔ Any combination of LED + mirror bandwidth could be selected.

From cancer cells to refractometry

- Applying voltage causes blue-shift; consistent with T; concern with cell viability

- Develop method with air holes and cavity length interpolation to separate $n \cdot L$
- Measure n(T) for PBS and water with custom built isothermal apparatus
- $n_{water}(T)$ disagrees with NIST, consider mirror penetration
- $n_{PBS}(T,\lambda)$ with a spatial resolution, useful for quantifying refractive index or temperature

Lab refractometers

- Bausch & Lomb Abbe-3L
- T dependence, λ=589nm
- Thanks to Dr. Tracy Perkins

- Atago DR-M2/1550
- Both T and λ dependence
- ~$18k (sans circulating bath)

http://chemlab.truman.edu/CHEMLAB_BACKUP/PChemLabs/CHEM324Labs/LiquidVapor/Refractometer.htm
http://www.atago.net/english/products_multi.php

Microfluidic FP refractometers

- Microfluidic refractometers integrate well with "lab-on-a-chip" devices, which are common for biological samples.
- The resonant wavelengths of a Fabry-Pérot (FP) optical cavity are highly dependent on the optical path length ($n \cdot L$) inside the cavity.
- Any method utilizing an FP cavity for refractometry will need to separate refractive index and the physical cavity length. A few ways get around this separation are:
  - Measure only Δn
  - Measure λ_m vs. known n ➔ calibration curve
  - Measure $n_1 = n_0 * (\lambda_{m1} / \lambda_{m0})$
- However, these methods depend on a fixed cavity length. Cavity length may change by thermal expansion or polymer swelling.

P. Domachuk *et al*, 2006

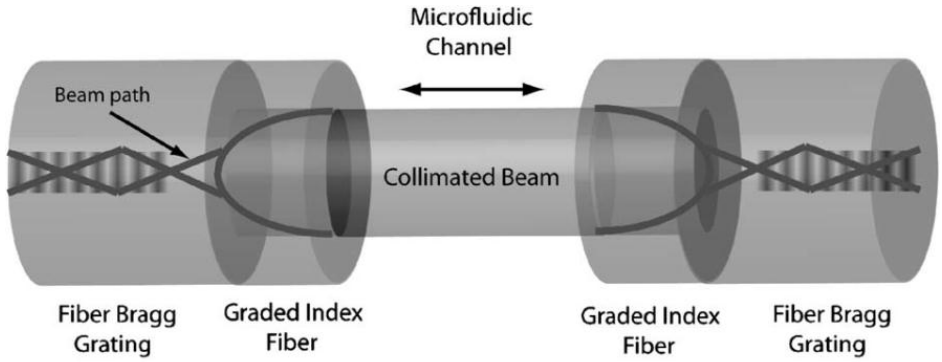

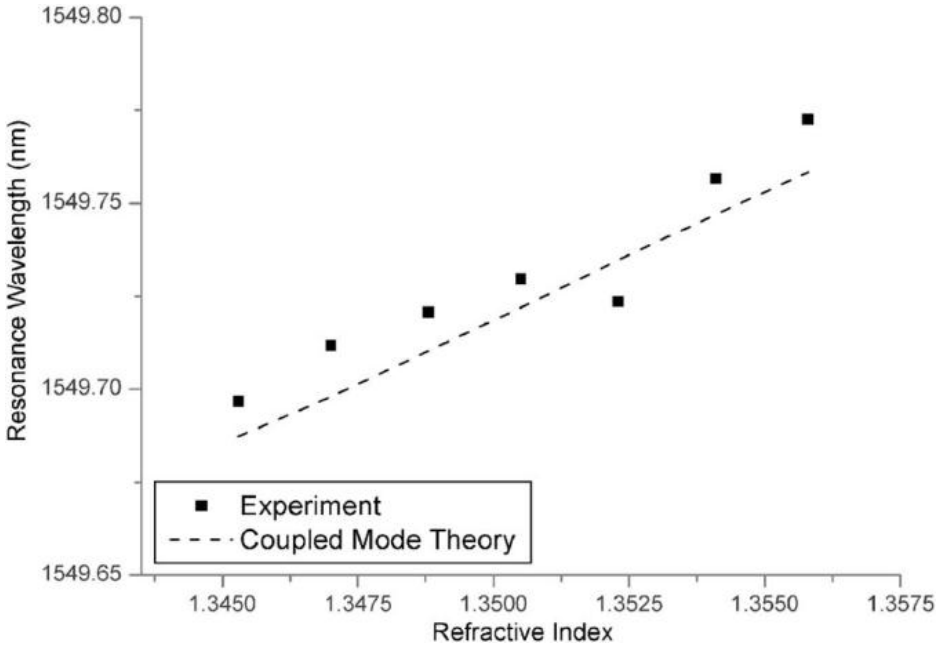

P. Domachuk *et al*, *Appl. Phys. Lett.*, 88, 093513 (2006).

R. St-Gelais *et al*, 2009

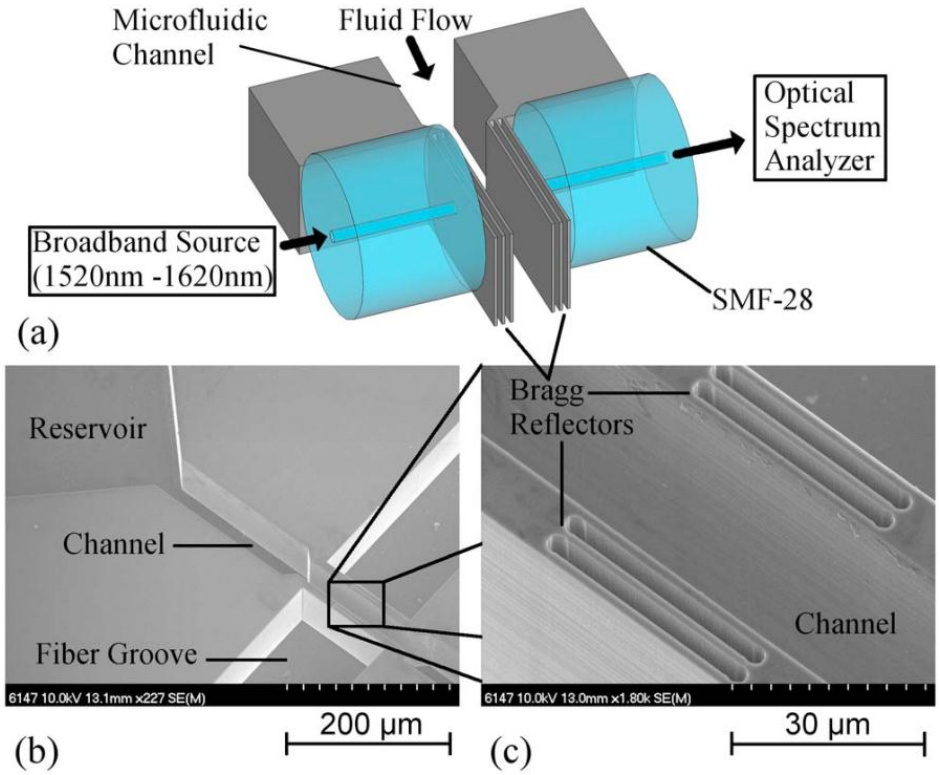

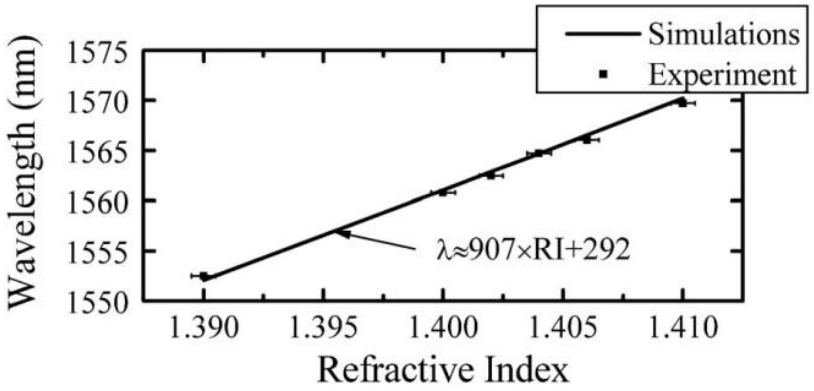

R. St-Gelais *et al*, *Appl. Phys. Lett.*, 94, 243905 (2009).

L. K. Chin *et al*, 2010

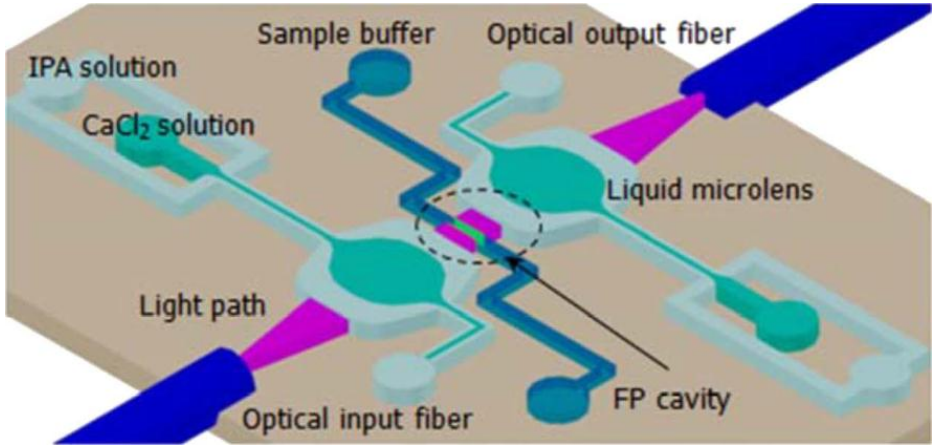

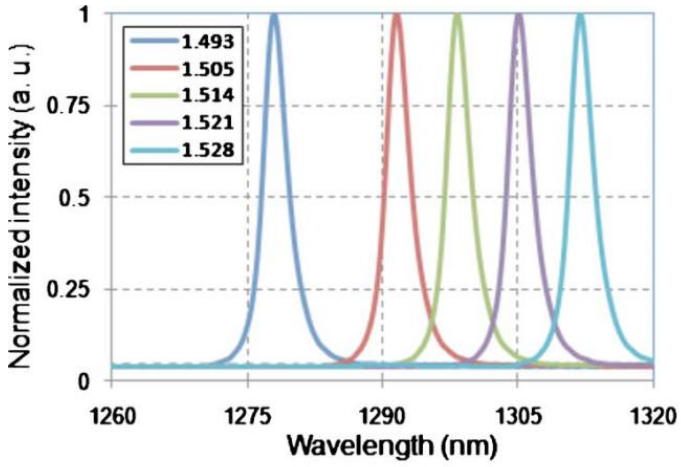

(a)

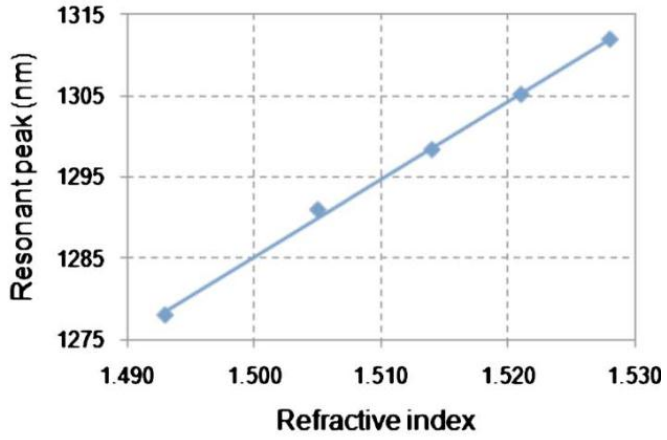

(b)

L. K. Chin *et al*, *Biomicrofluidics*, 4, 024107 (2010).

Outline

- Motivation and background
- Computer modeling
  - Electrostatics
  - Joule heating
  - Mirror penetration
- Experimental materials and methods
- Experimental results
- Summary

Electrostatic geometry (2D)

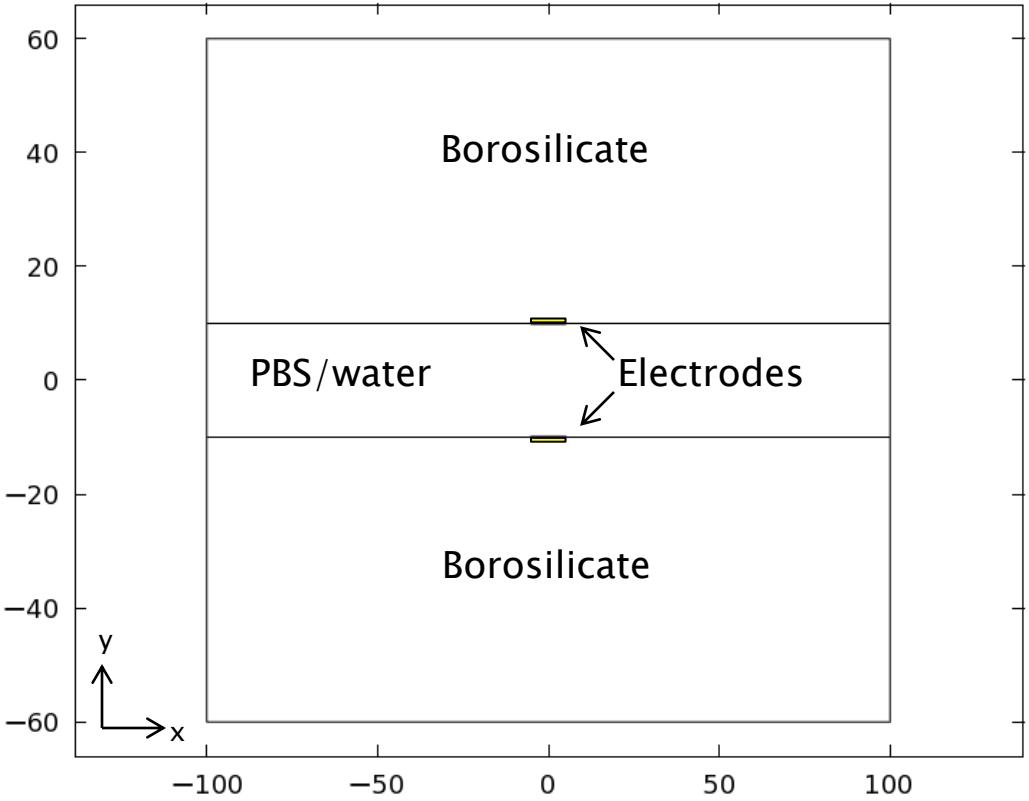

E-field results

Planar electrodes

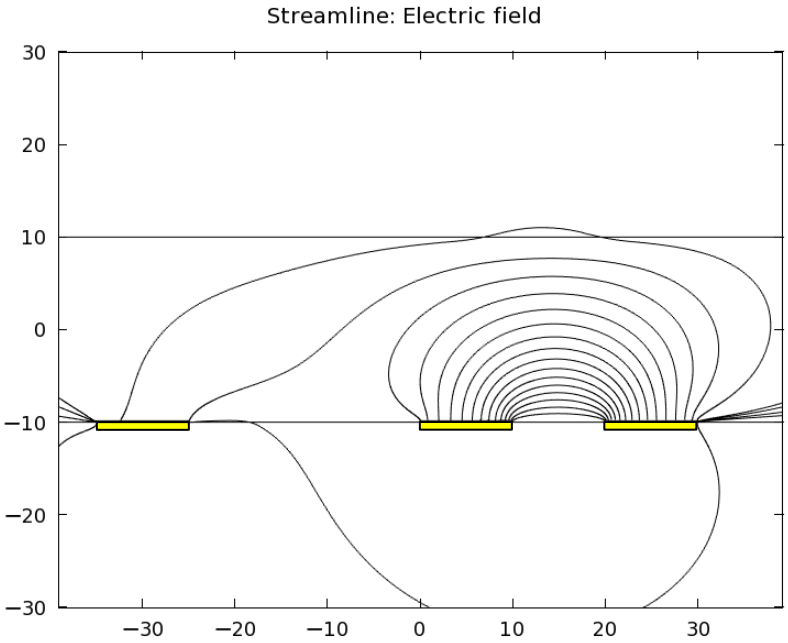

Top and bottom electrodes

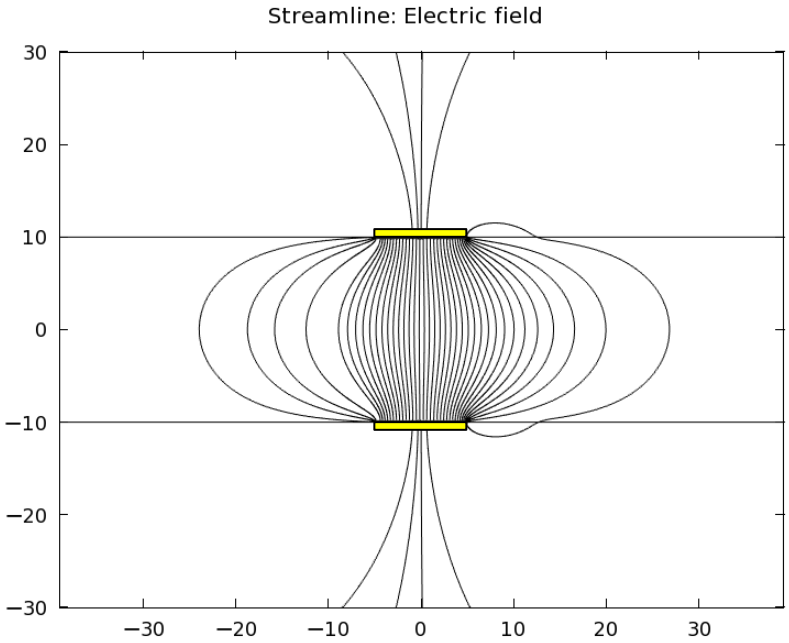

- Electrodes are drawn in for illustrative purposes.
- When a particle is exposed to an electric field, a dipole is induced. If the field is non-uniform, a dielectrophoretic (DEP) force acts on the particle.
  - The DEP force is proportional to the gradient of the electric field squared.
  - A nDEP vs pDEP force will depend on the CM factor.

E^2 and $|\nabla(E^2)|$ at center of channel

Planar electrodes

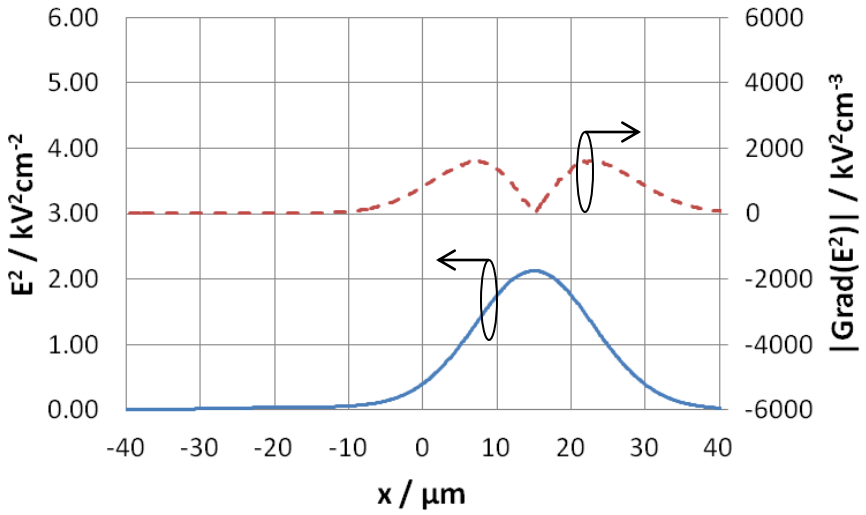

Top and bottom electrodes

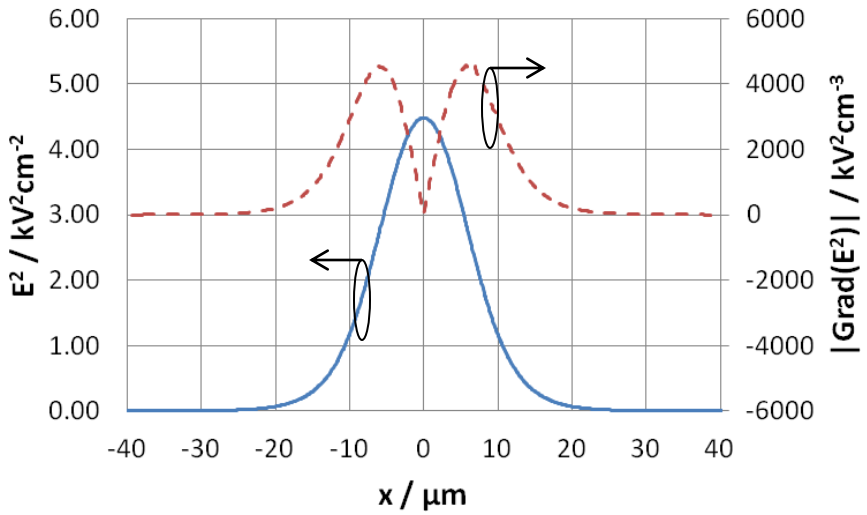

- Top and bottom electrodes:
  - Maximum $|\nabla E^2|$ is 2.8x bigger than planar electrodes.

  ➔ Good, since the DEP force is proportional to $|\nabla E^2|$

  - Maximum E^2 is 2.11x bigger than planar electrodes.

  ➔ Bad, since the joule heating source term is $Q = \sigma E^2$

Joule heating geometry (3D)

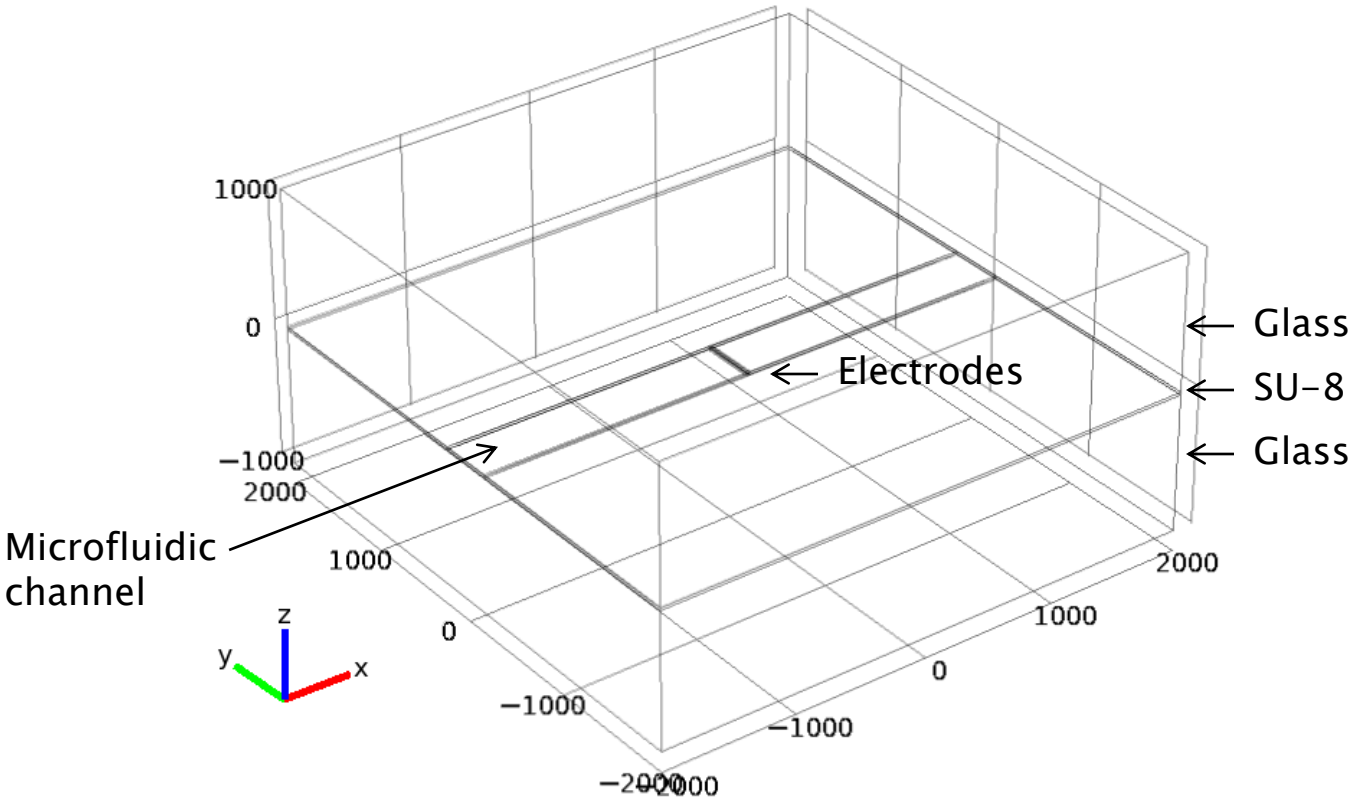

Temperature dependent parameters

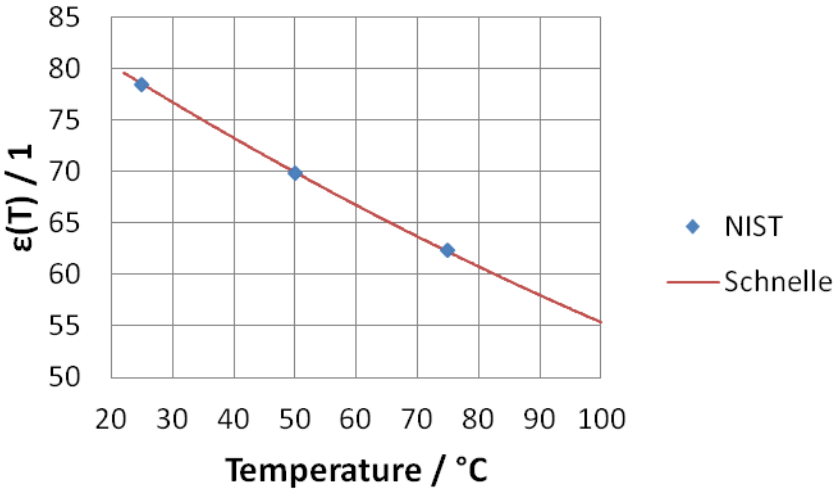

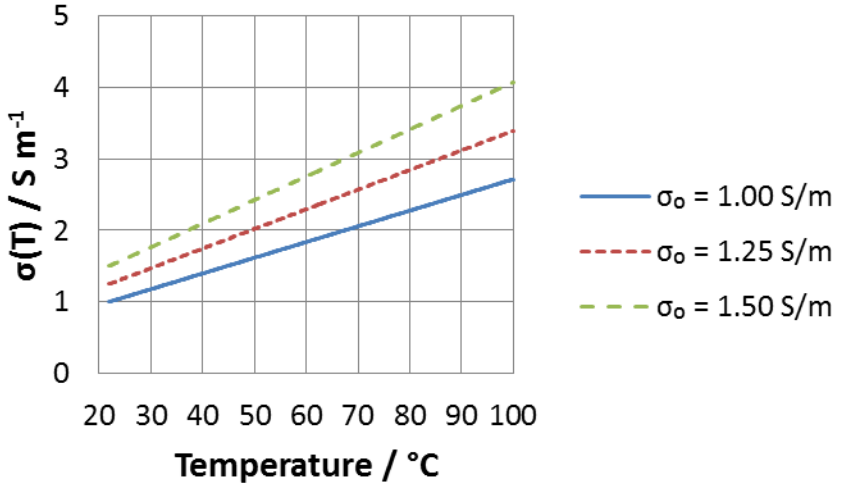

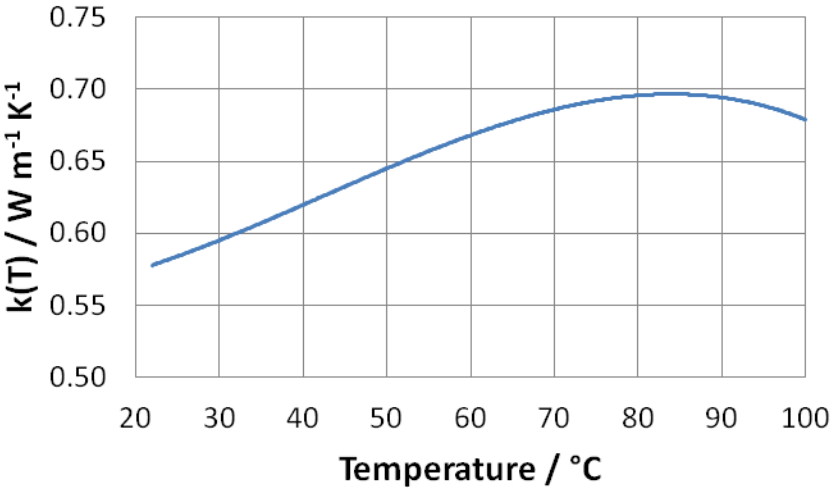

- ➔ Simulations provide easy "black box" implementation of an otherwise a difficult analytic solution.
- ➔ Simulations are additionally useful for finding a temperature distribution.

T. Schnelle *et al*, *Journal of Electrostatics*, vol. 47, no. 3, 1999.
M. Uematsu and E. U. Franck, *J. Phys. Chem. Ref. Data*, vol. 9, no. 4, 1980.

Joule heating mesh

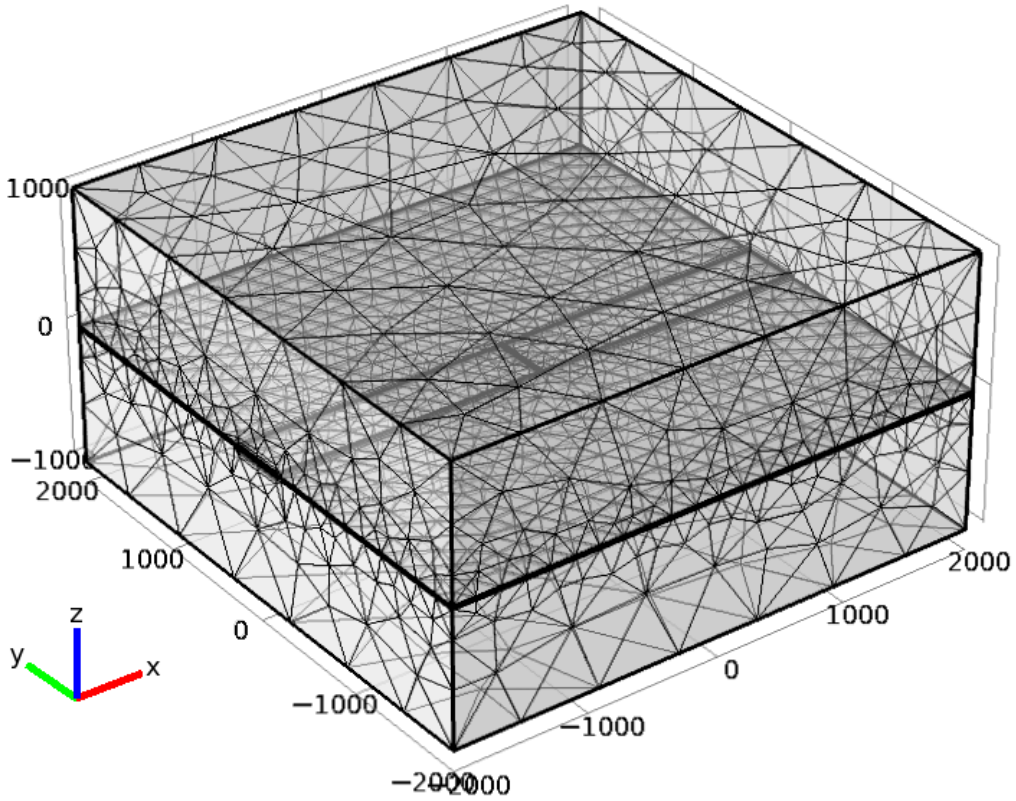

The art of 3D meshing

- A 3D mesh results in many more mesh elements, and COMSOL will produce an out-of-memory error message with too many elements (~30,000 on main computer).
  - **Problem**: Many elements are needed so the mesh isn't a variable.
  - **Partial fix**: Add boundary meshes in 2D planes near the electrodes.

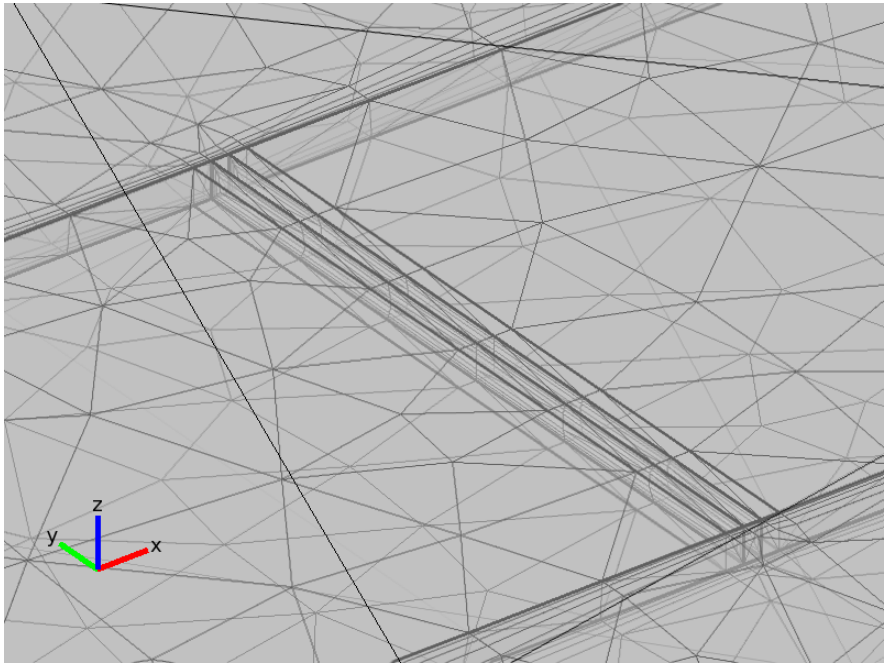

Meshing with different computers

	Main computer	Other computer1	Other computer2
Comsol version	4.1	4.2	4.2
Computer specs	Intel Pentium 4, 768MB or 2GB Ram, 32-bit OS	Intel Core i7, 6GB Ram, 64-bit OS	Intel Core i7, 6GB Ram, 64-bit OS
Custom or pre-defined mesh	Custom	Pre-defined: Normal	Pre-defined: Finer
# elements	29,966	238,330	556,136
DoF	126,592	809,612	1,784,100
Time	164s (~3min)	128s (~2min)	1433s (~24min)

- Work was done on Main computer.

Meshing with different computers

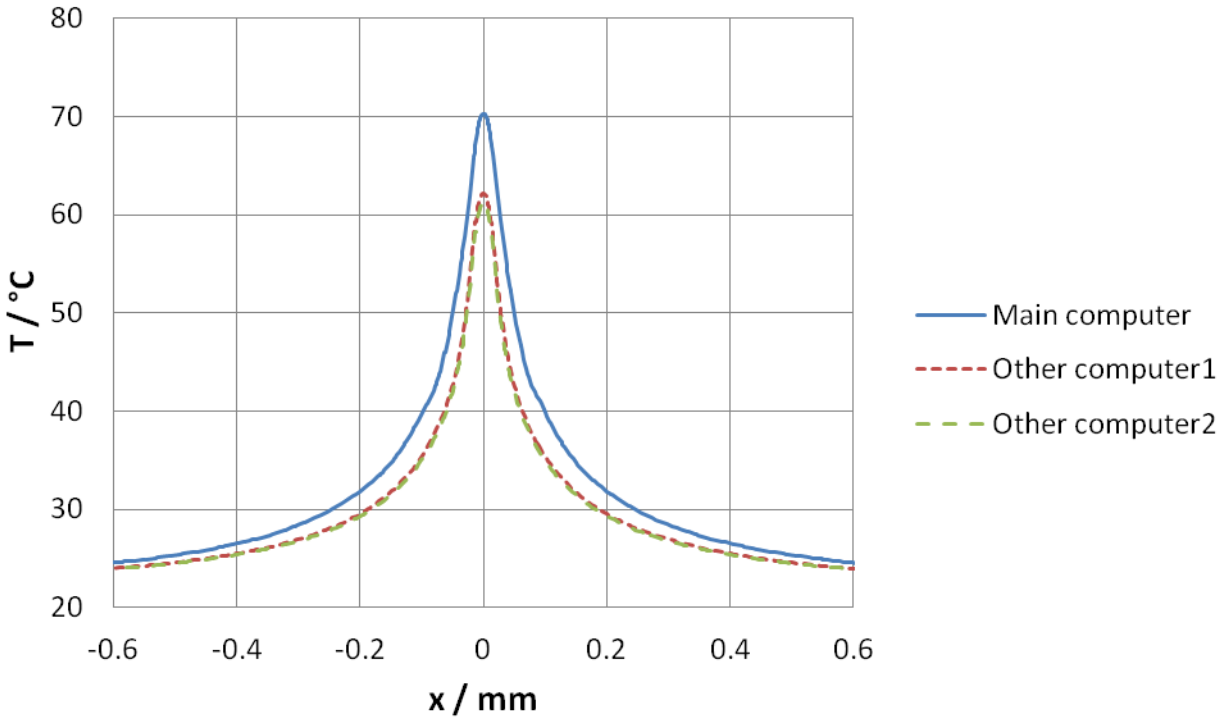

- x-data is at the center of the microfluidic channel (y=0, z=0)
- Difference at the maximum temperature is 9°C
- Scaling factor of (Other computer2)/(Main computer) = 0.87

Borosilicate vs. sapphire glass

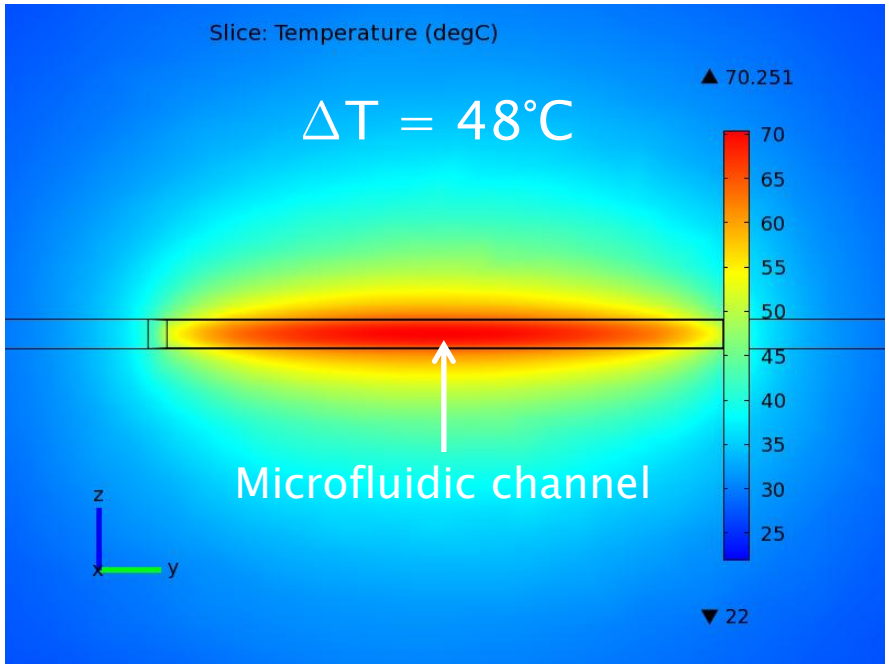

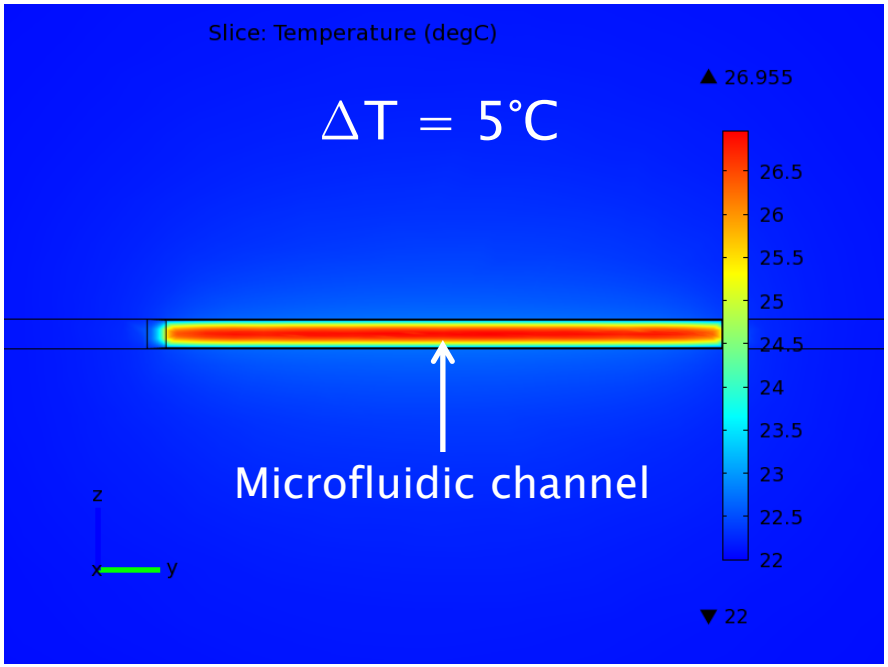

- **Advantages**:
  - Lower thermal conductivity, allowing big temperature gradients (optics).
  - Uses a higher quality mirror from a commercial vendor.

- **Advantage**:
  - Higher thermal conductivity, which reduces temperature rises that can be lethal to biological cells (biology).

Thanks to Dr. Kisker for suggestion of sapphire glass.

Mirror penetration depth

- Penetration depth is the length in the mirror at which the light appears to reflect, or the energy falls to $1/e$ of its initial value.

- Needs to be considered in FP cavities with dielectric mirrors, QWMs, DBRs.

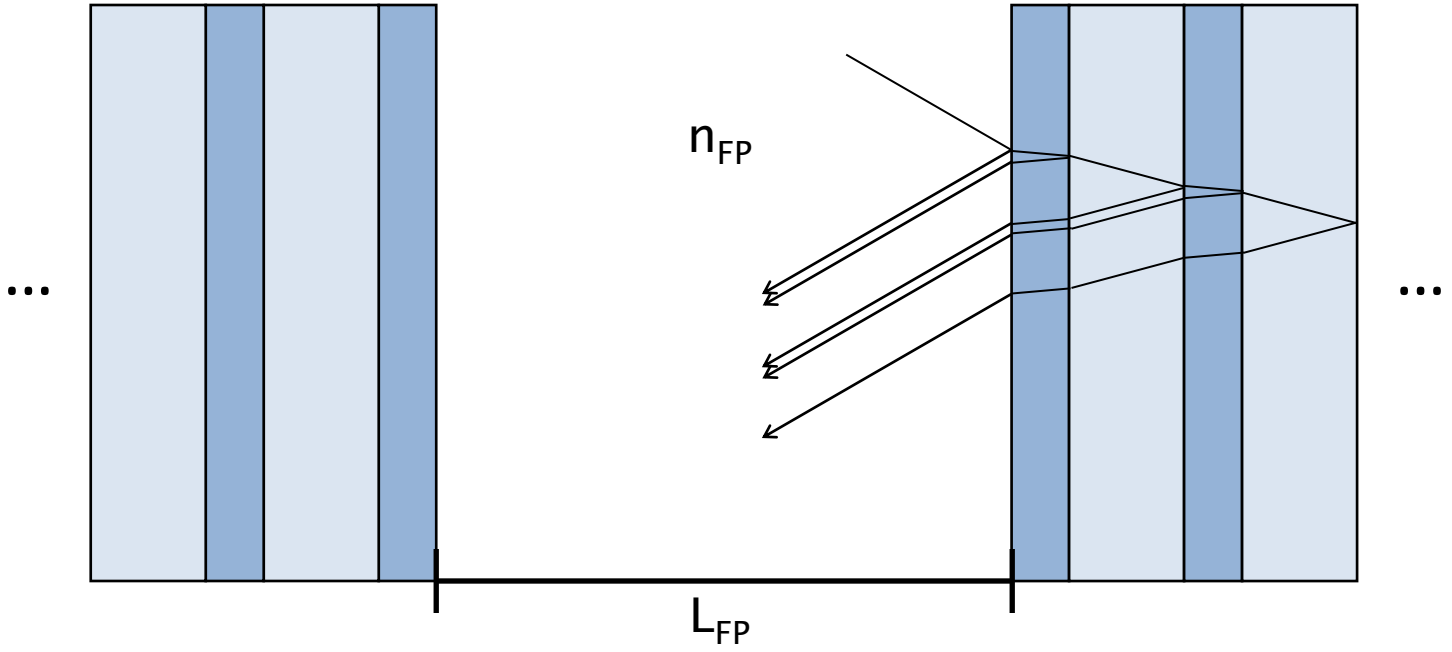

D. I. Babic and S. W. Corzine, *IEEE J. Quantum Electron.*, vol. 28, no. 2, 1992.

Mirror reflectivity with TFCalc

“Hard”

HIGH, n = 9.1500

SiO_2, n(λ=886nm) = 1.452

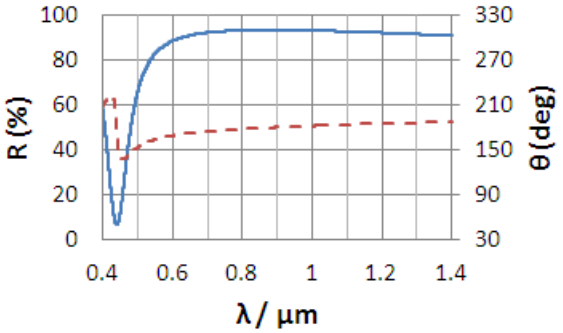

“Our”

HfO_2, n(λ=888nm) = 1.889

…

SiO_2, n(λ=886nm) = 1.452

HfO_2, n(λ=888nm) = 1.889

SiO_2, n(λ=886nm) = 1.452

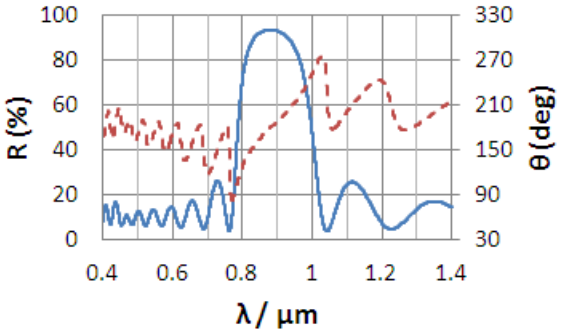

“Soft”

HIGH, n = 1.670

…

LOW, n = 1.450

HIGH, n = 1.670

SiO_2, n(λ=886nm) = 1.452

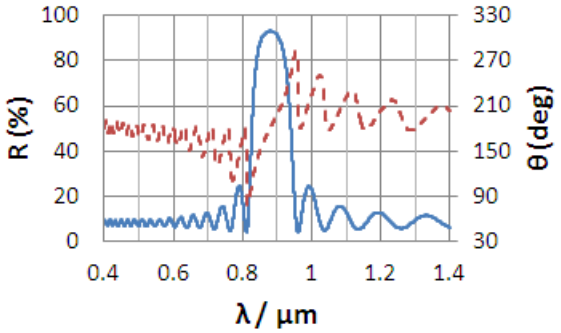

FP transmission with TFCalc

- At the mirror center wavelength (λ_0 = 880nm), there is no mirror penetration.
- Mirror penetration becomes greater at resonant wavelengths further away from λ_0.

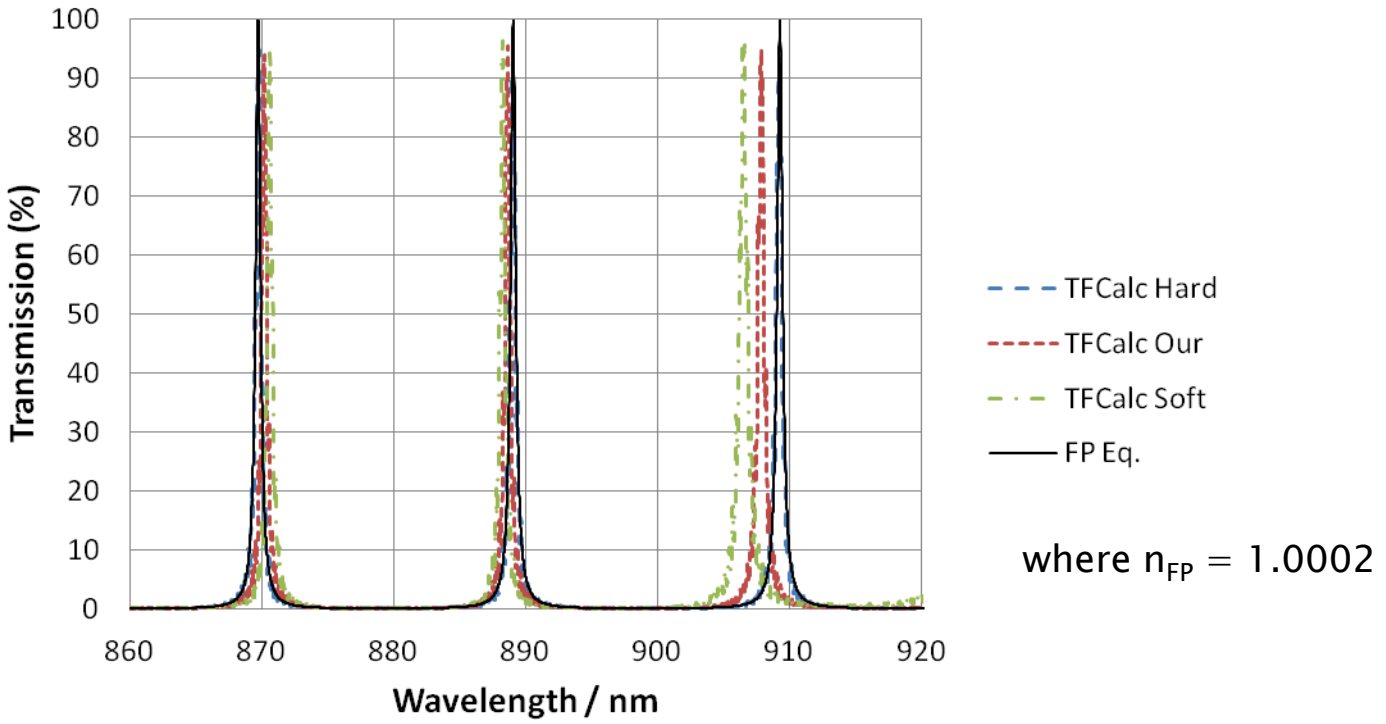

where n_{FP} = 1.0002

Original and modified cavity phase

- Original: $2\beta_m(L_{FP}+2L_\tau)-2\omega_o\tau=2\pi m,$ $\beta_m=n_{FP}\omega_m/c,$ $\tau=2n_{FP}L_\tau/c$
- Modified: $2\beta_m(n_{FP}L_{FP}+2L_\tau)-2\omega_o\tau=2\pi m,$ $\beta_m=\omega_m/c,$ $\tau=2L_\tau/c$

$$L_\tau=c\tau/2$$

Get same values as Garmire's Eq.

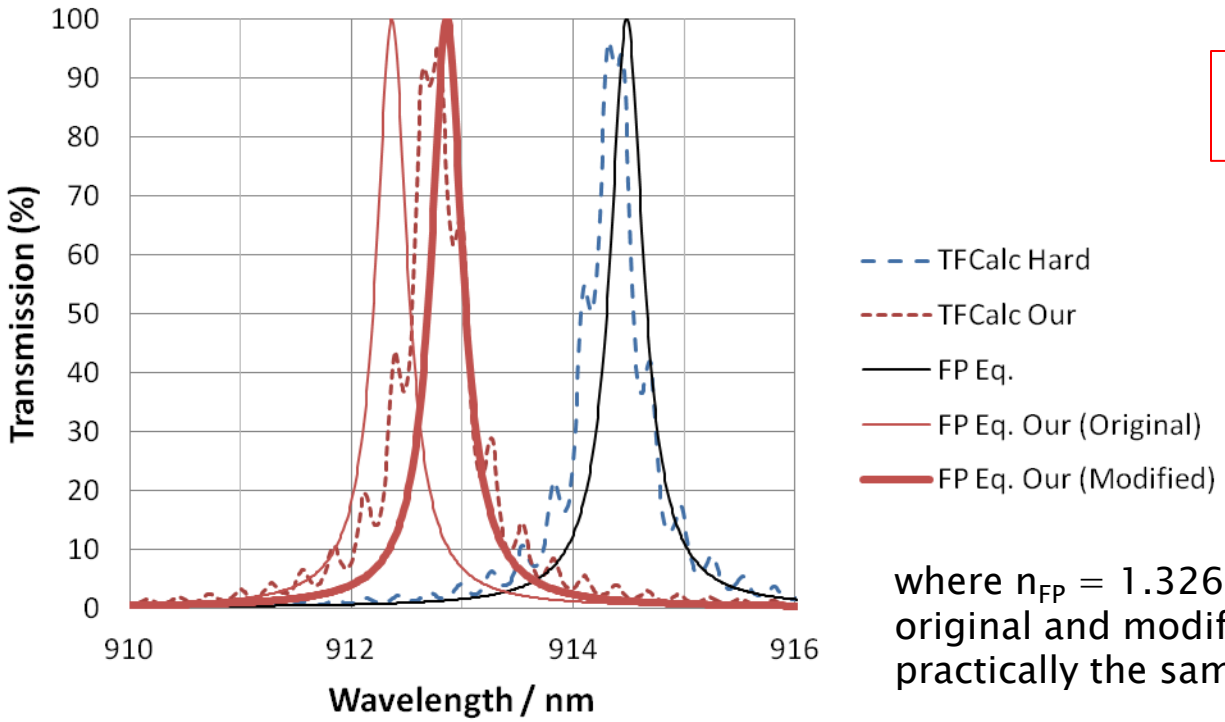

where n_{FP} = 1.326. If air in cavity, original and modified equations are practically the same.

D. I. Babic and S. W. Corzine, *IEEE J. Quantum Electron.*, vol. 28, no. 2, 1992.
E. Garmire, *Applied Optics*, vol. 42, no. 27, 2003.

Outline

- Motivation and background
- Computer modeling
- Experimental materials and methods
  - OFIS chip
  - FP spectra with spatial resolution
  - Algorithm for obtaining refractive index
- Experimental results
- Summary

OFIS Chip

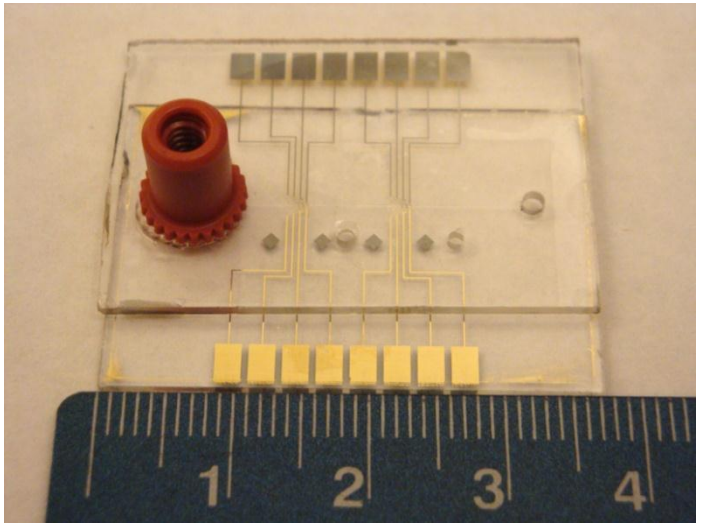

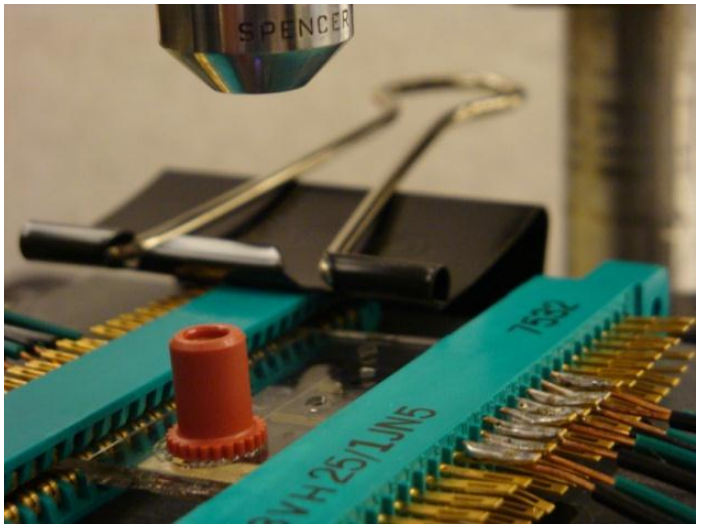

FP spectra with spatial resolution

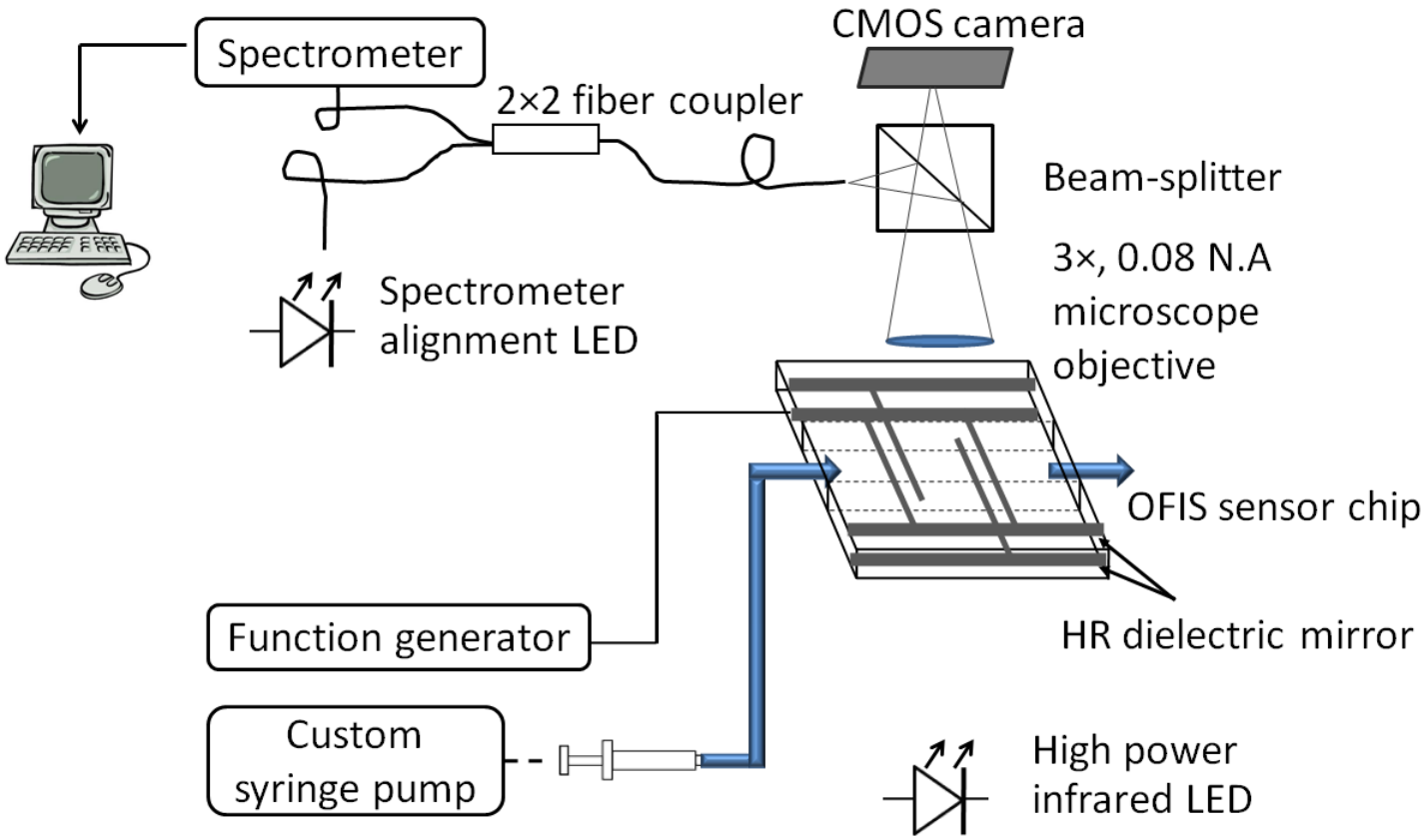

- The fiber and objective lens act as a spatial filter resulting in a spot size of approximately 62.5μm/3 = 21μm. This is the spatial resolution.
- The alignment LED shows where the spot is located.

Data processing algorithm for L_{interp}

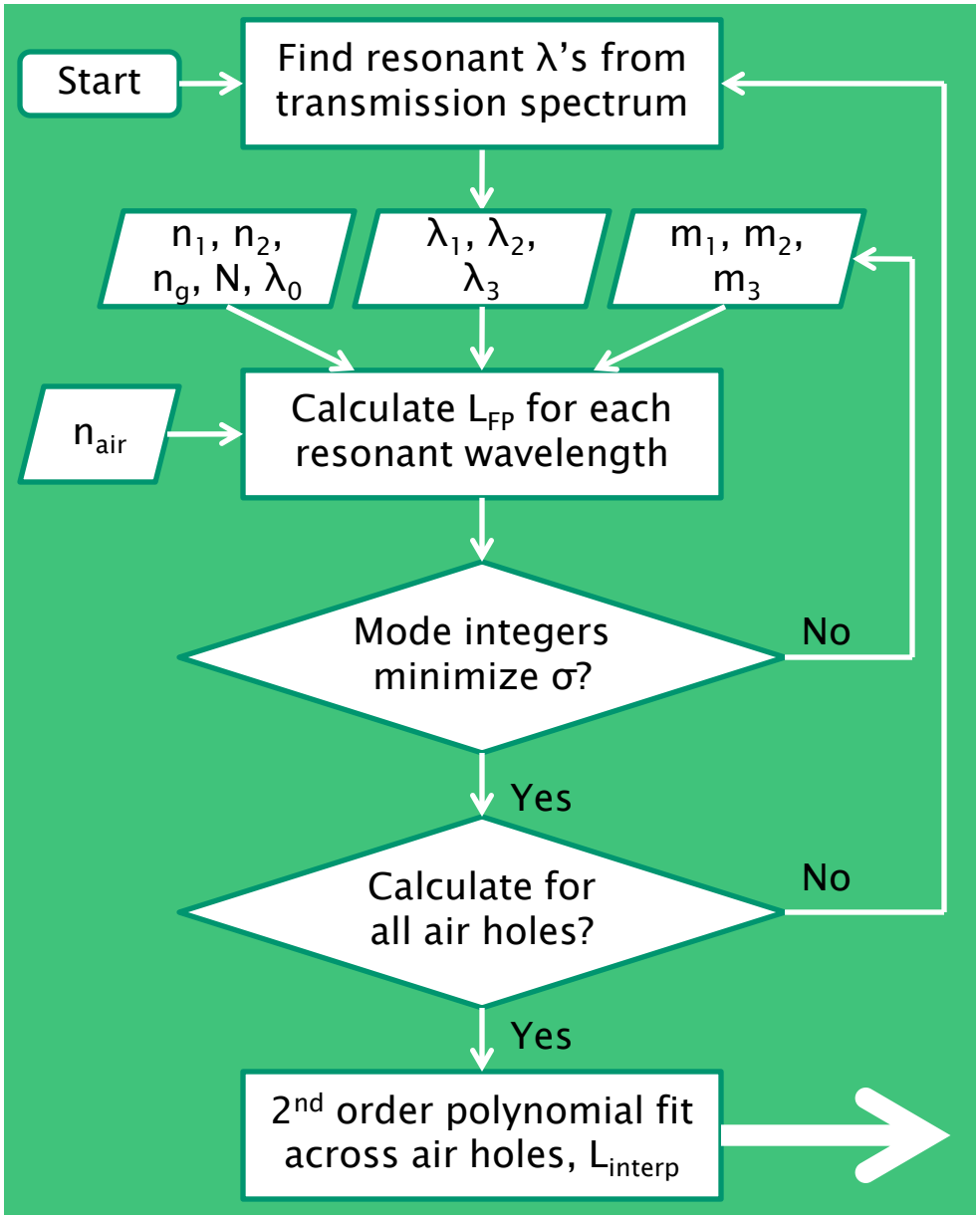

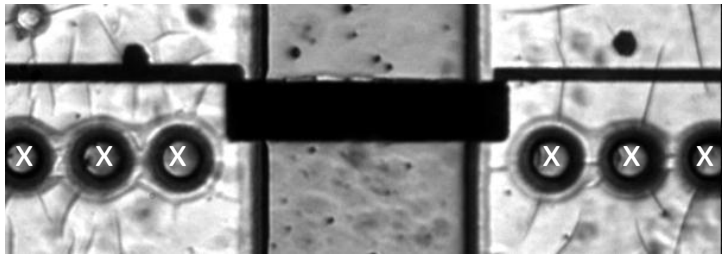

$$L_{FP} = \frac{m\lambda_m}{2n_{FP}} + \frac{2L_\tau}{n_{FP}}\left(\frac{\lambda_m}{\lambda_0} - 1\right)$$

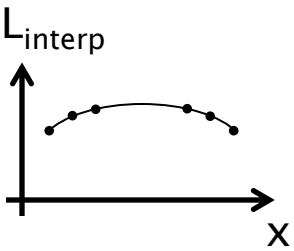

Data processing algorithm for RI

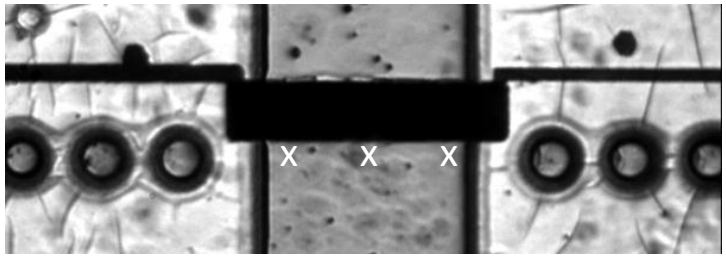

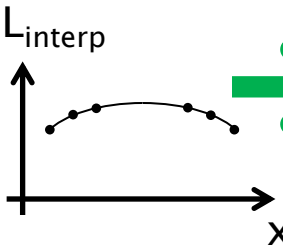

Find resonant λ's from transmission spectrum

n_1, n_2, n_g, N, λ_0

λ_1, λ_2, λ_3, λ_4

m_1, m_2, m_3, m_4

Calculate n_{FP} for each resonant wavelength

Mode integers minimize σ?

No

Yes

Calculate for all points?

No

Yes

n(λ_1), n(λ_2), n(λ_3), n(λ_4)

Finish

$$n_{FP} = \frac{m\lambda_m}{2L_{FP}} + \frac{2L_\tau}{L_{FP}}\left(\frac{\lambda_m}{\lambda_0} - 1\right)$$

$$L_\tau(n_{FP})$$

➔ 3rd order polynomial

➔ linear approximation

There is an instance in the data where two sets of mode integers both get close to minimizing σ…

Outline

- Motivation and background
- Computer modeling
- Experimental materials and methods
- Experimental results
  1) Isothermal apparatus
  2) Joule heating
  3) GRIN lenses
- Summary

1) Isothermal apparatus

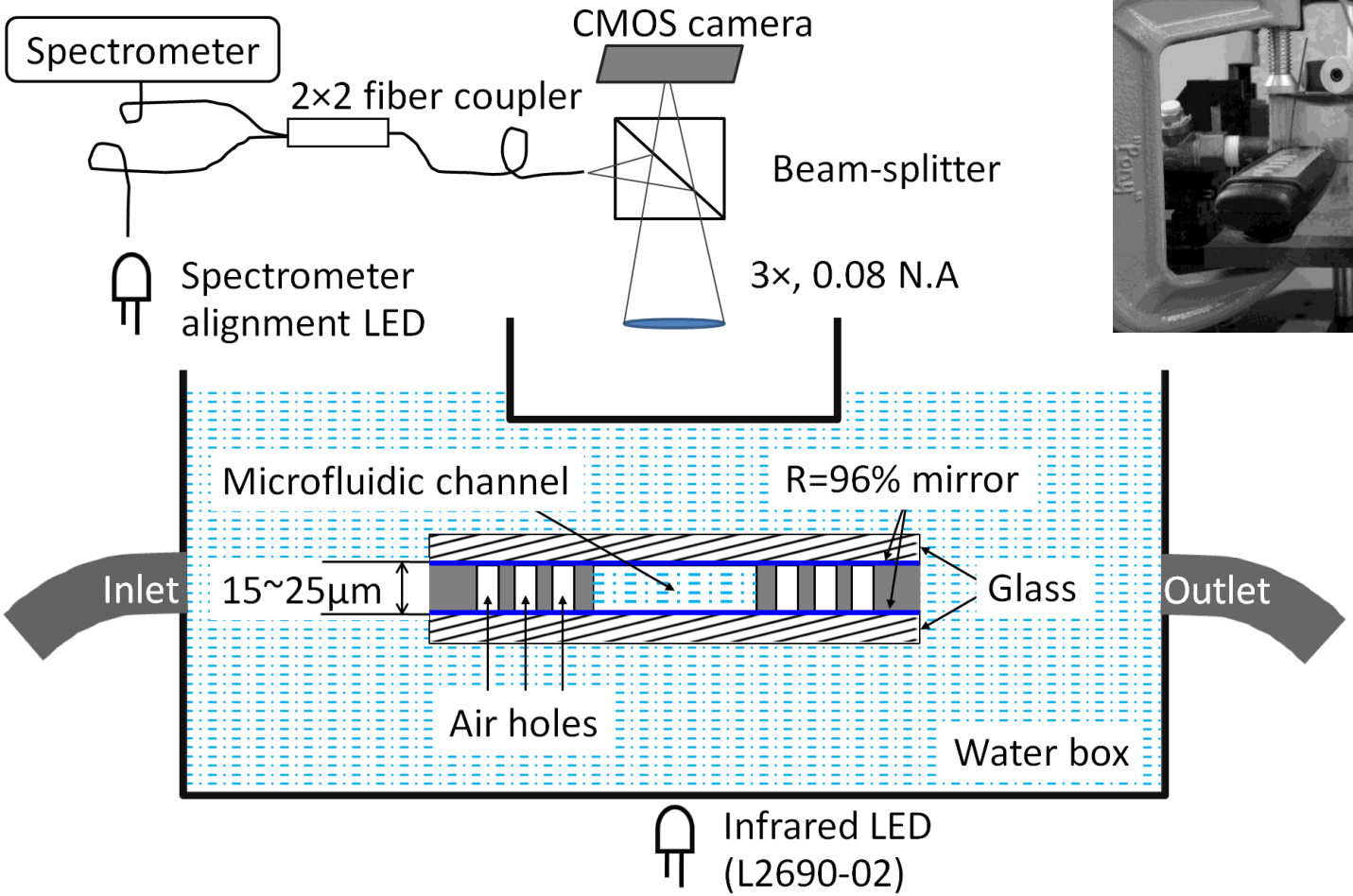

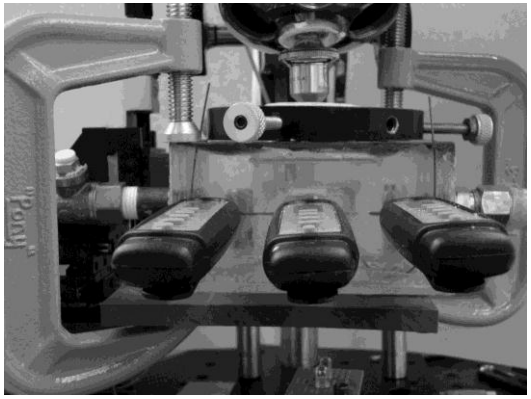

Isothermal apparatus details

- Temperature changes by about 1°C/min:
  - Increasing temperature was done by heating element in water bath.
  - Decreasing temperature was done by adding cups of cold water.
  - All spatial points are measured at one temperature.
  - Temperature pattern: 30°C, 50°C, 40°C, 70°C, 60°C.

- Temperature on the water bath was adjusted to reach the desired temperatures on the thermometers.
  - The standard deviation between the 3 thermometers was $\leq$ 0.3°C
  - At hotter temperatures, the water bath needed to be slightly higher to obtain the desired temperature on the thermometers.

- The time needed to measure at one temperature is ~45min-1hr:
  - 15 points were often measured (12 air holes, 3 points in the channel) at a rate of ~2min/1 point ➔ 30min.
  - Additional time is needed for changing temperatures, and sometimes power cycling water bath.

Empirical choice of air holes

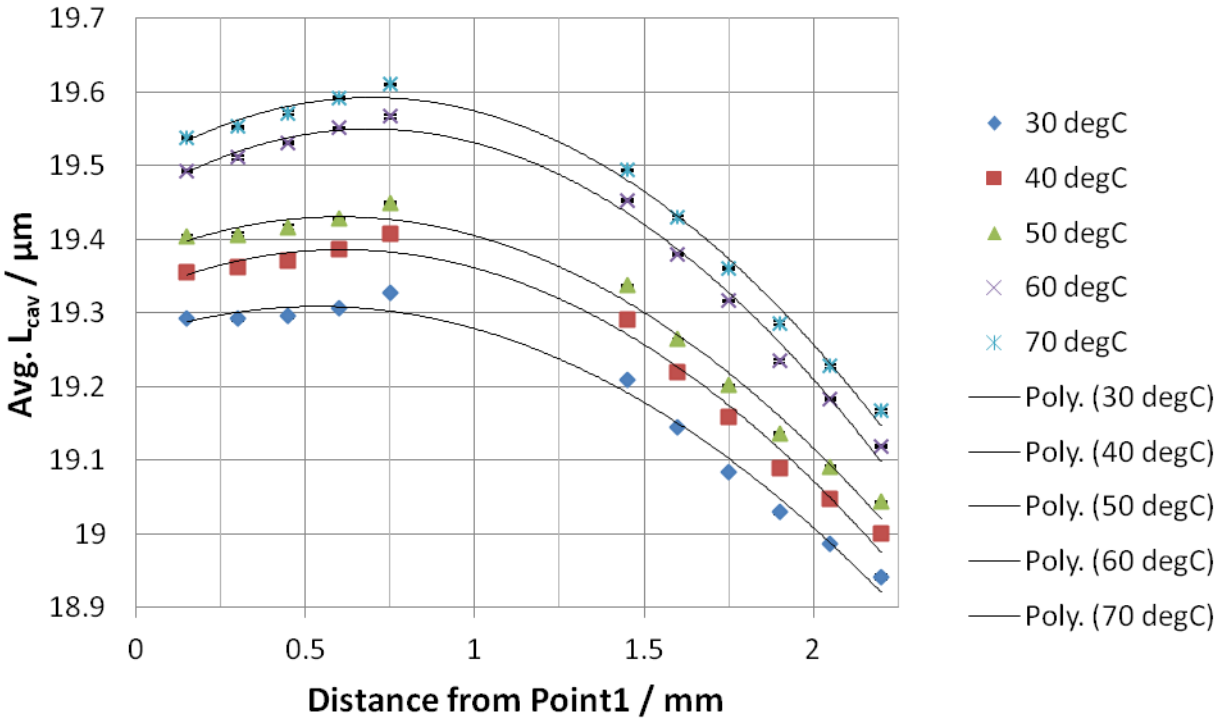

- It is better to use 3 air holes on each side of the channel:
  - Provides a better 2nd order polynomial fit of the swelled profile.
  - Allows for a possible obstructed air hole or water-filled air hole.

Chip 28-Jun-2011

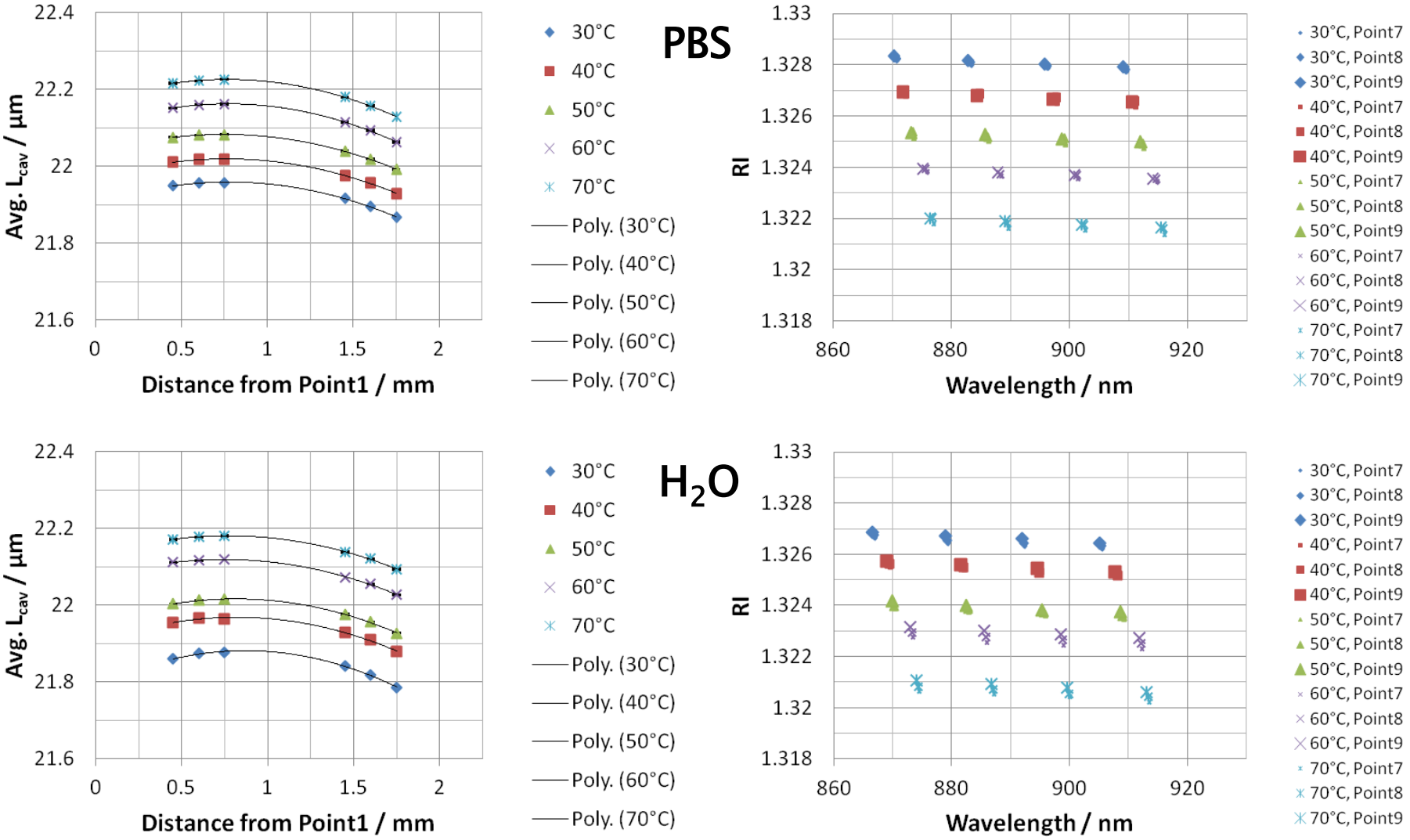

Chip 28-Jun-2011 H_2O vs. NIST

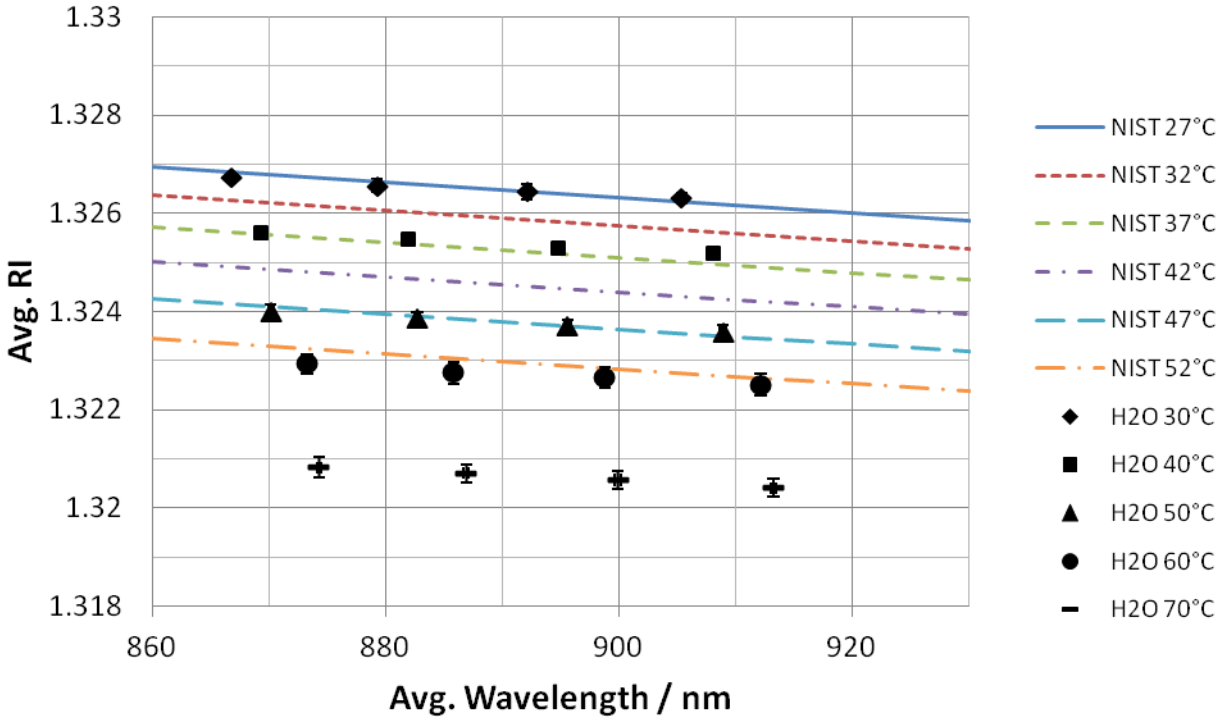

- The average and standard deviation use 3 spatial points.
- In general, RI values are higher than what is predicted by the NIST formula. The data at 60°C is especially higher.

A. H. Harvey *et al*, *J. Phys. Chem. Ref. Data*, vol. 27, no. 4, 1998.
W. Wagner and A. Pruß, *J. Phys. Chem. Ref. Data*, vol. 31, no. 2, 2002.

Justifying linear approximation n_{FP}

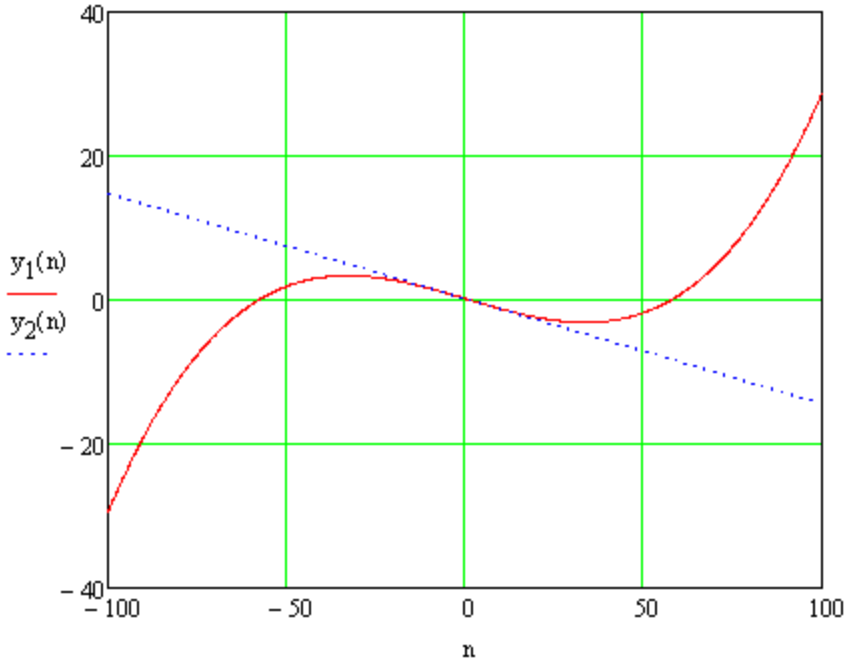

- Data used in this example is from Chip 28-Jun-2011, H_2O, 30°C, m=66, λ_m = 879nm.
- The linear approximation is good from n_{FP} = 1 to 2.

Chip 20-Aug-2011

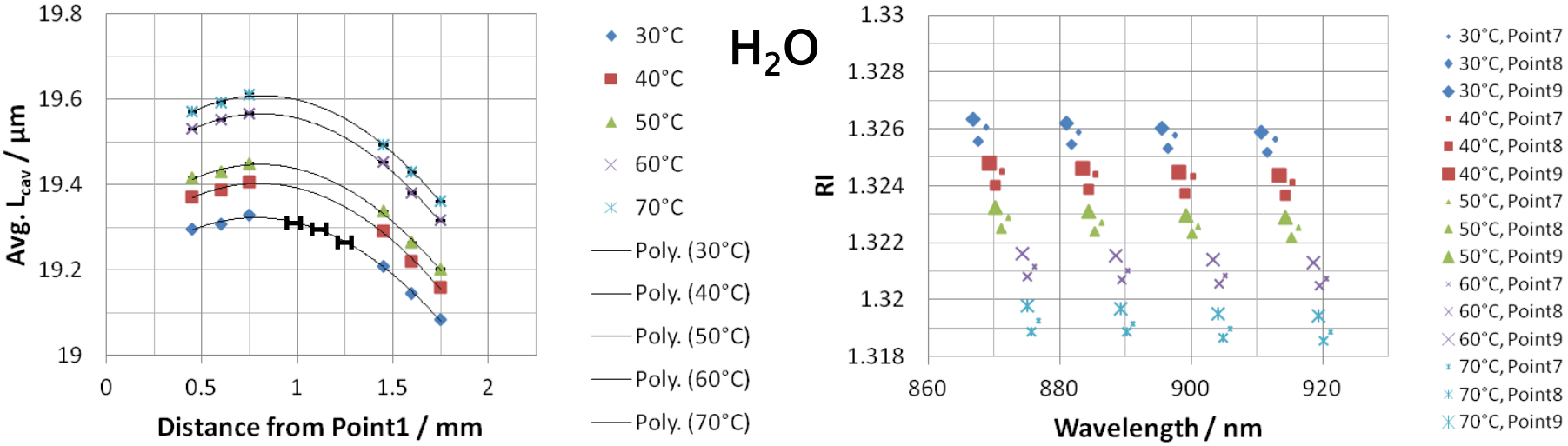

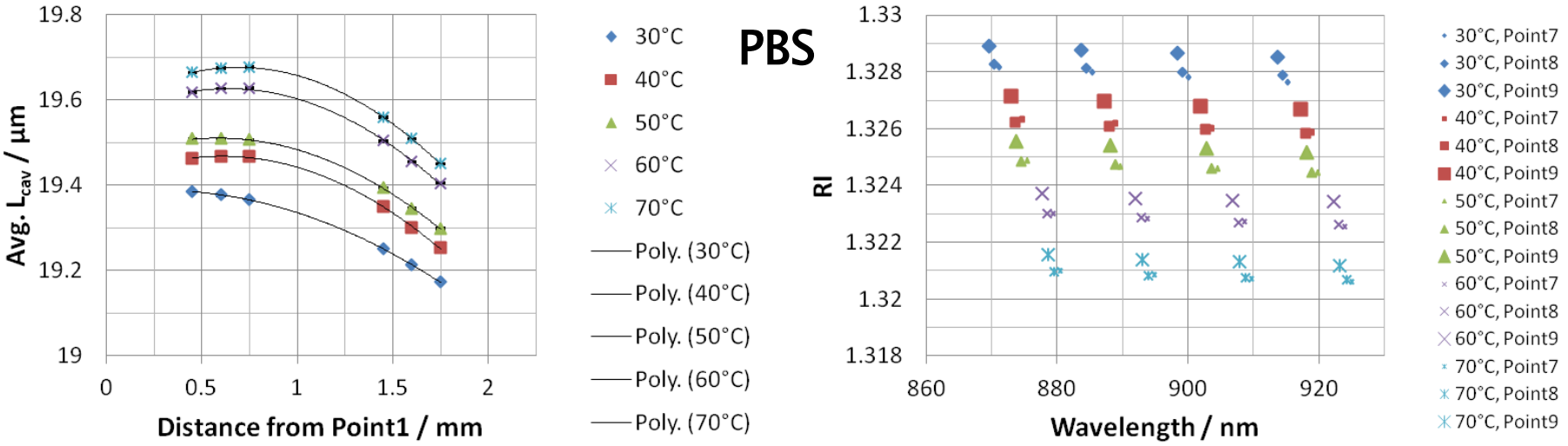

Chip 20-Aug-2011 H_2O vs. NIST

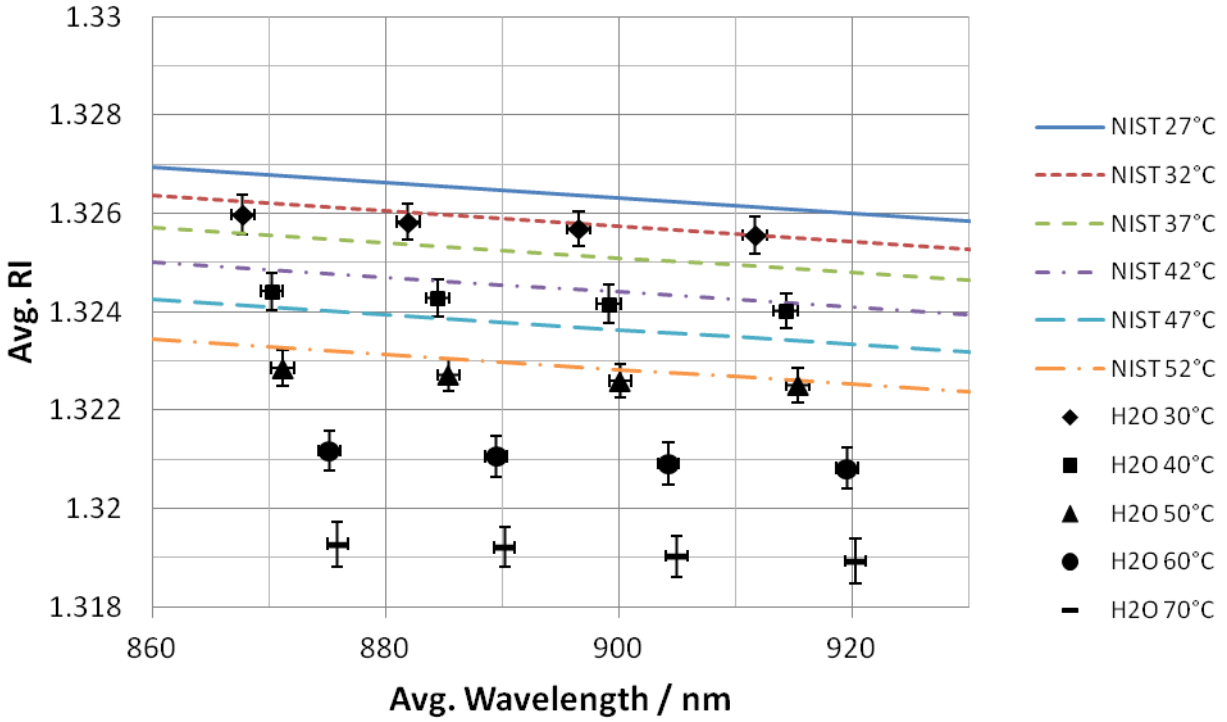

- The average and standard deviation use 3 spatial points.
- In general, RI values are lower than what is predicted by the NIST formula. This can be partially attributed to Points7&8 lowering the avg.

A. H. Harvey *et al*, *J. Phys. Chem. Ref. Data*, vol. 27, no. 4, 1998.
W. Wagner and A. Pruß, *J. Phys. Chem. Ref. Data*, vol. 31, no. 2, 2002.

Both chips, H_2O vs. PBS

Chip 28-Jun-2011

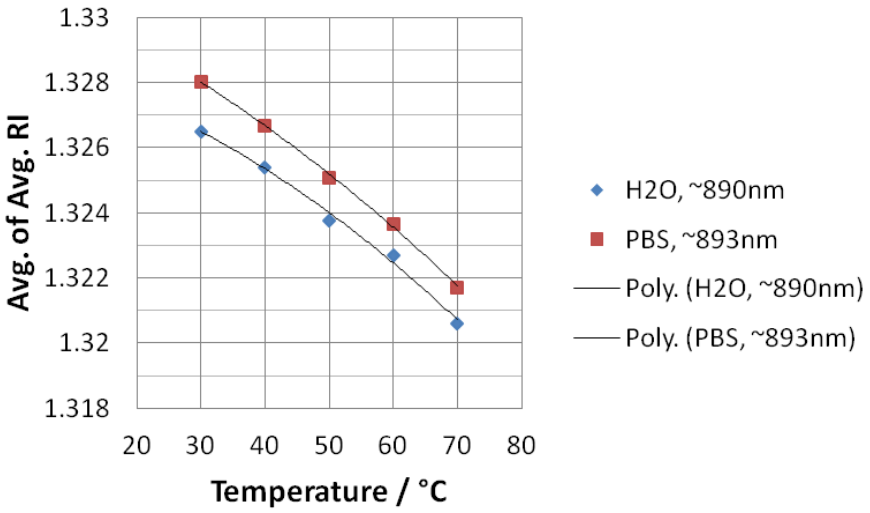

Chip 20-Aug-2011

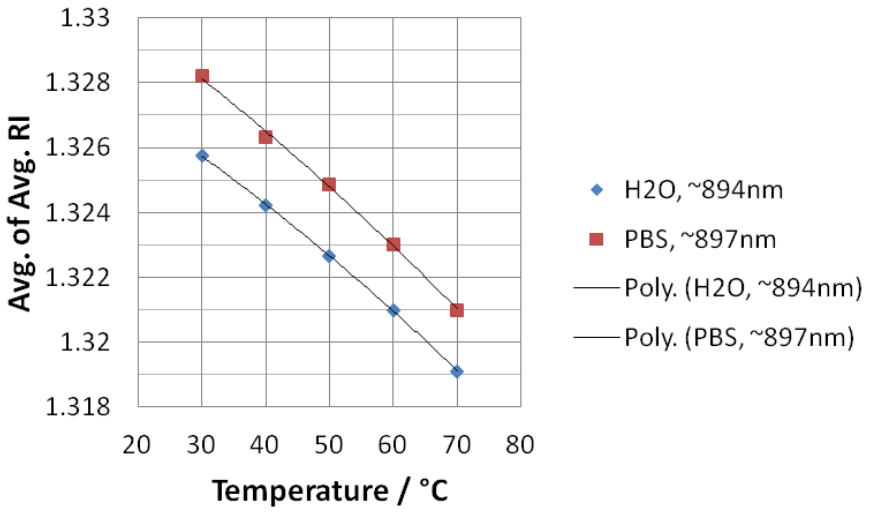

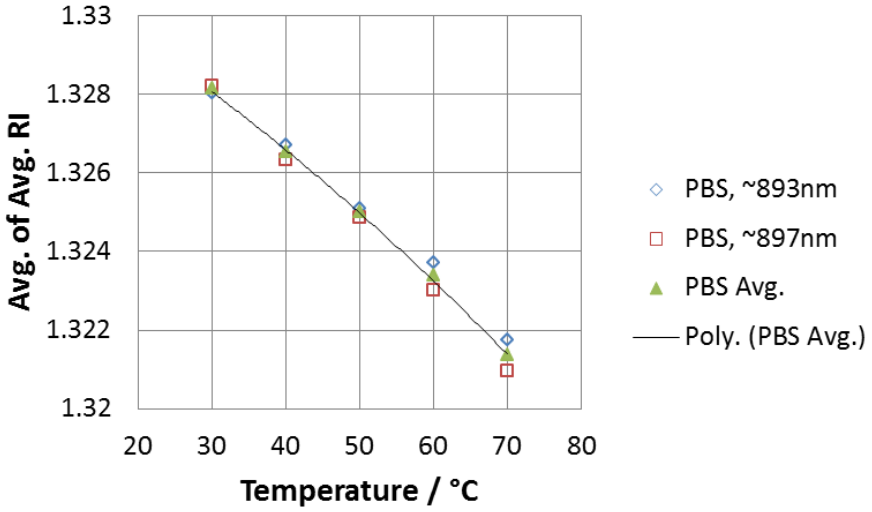

2) Joule heating, Chip 05-Apr-2011

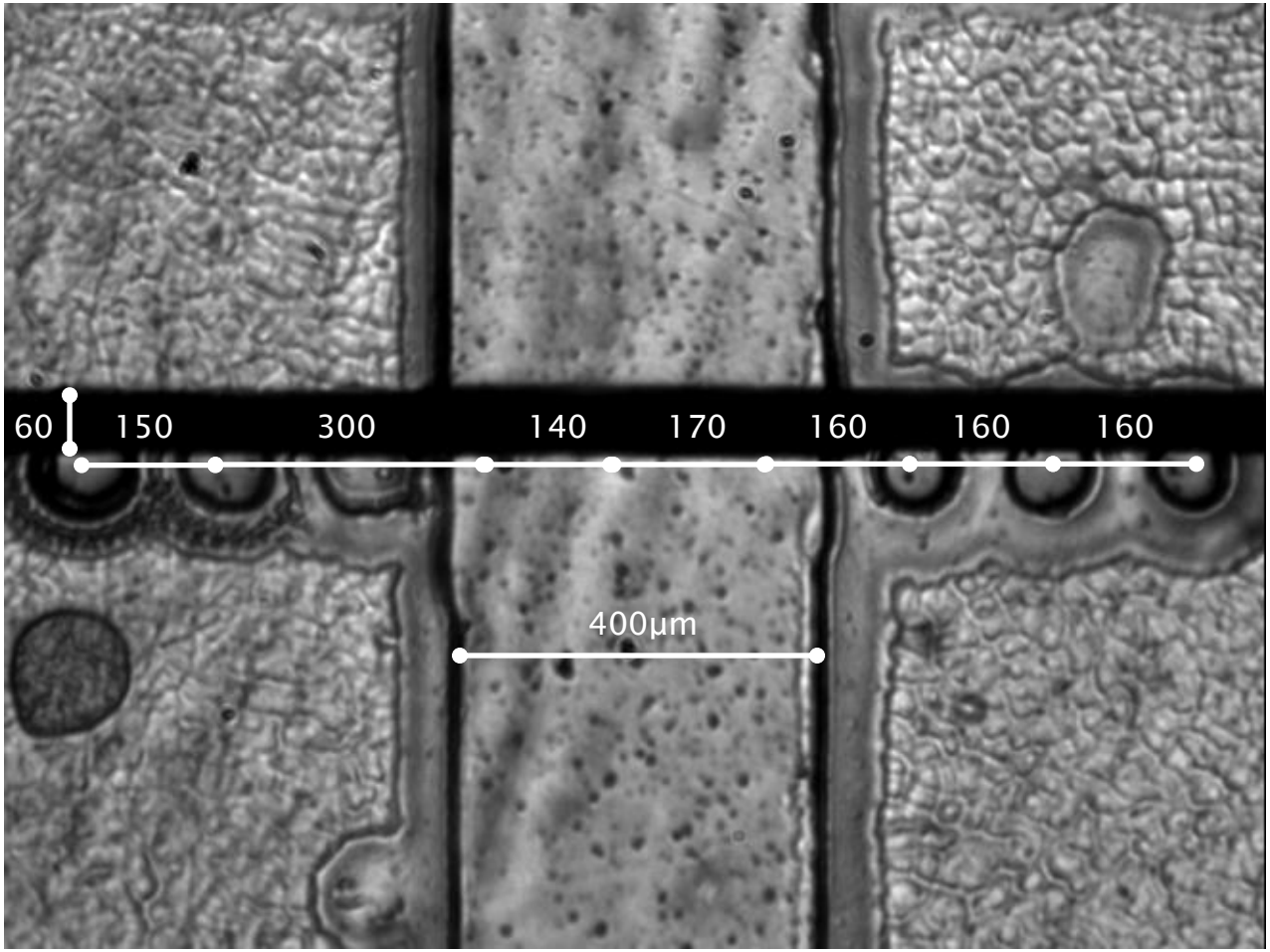

Joule heating, Chip 05-Apr-2011

- Each spatial point is measured with the electrodes off, turned on for 2 minutes, then turned off for two minutes.
  - The resonant wavelength nearly returns to the original position after the 4 minutes.
  - This is repeated for each point.

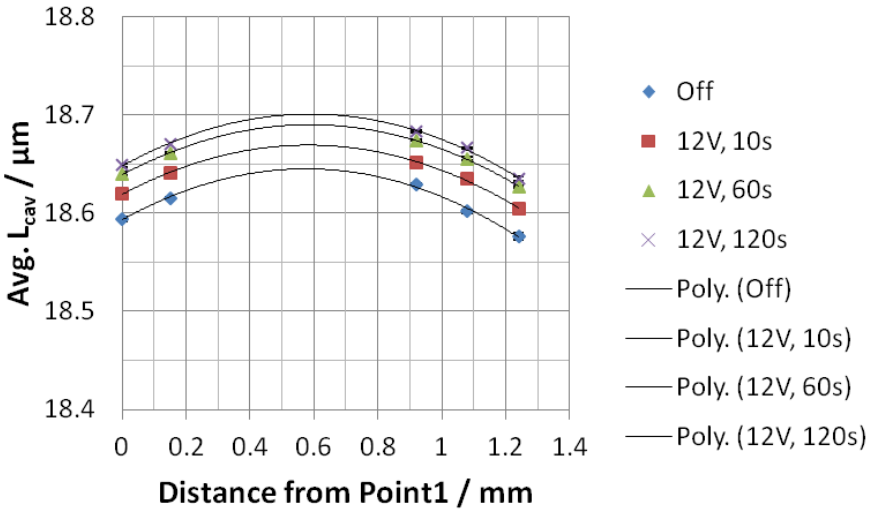

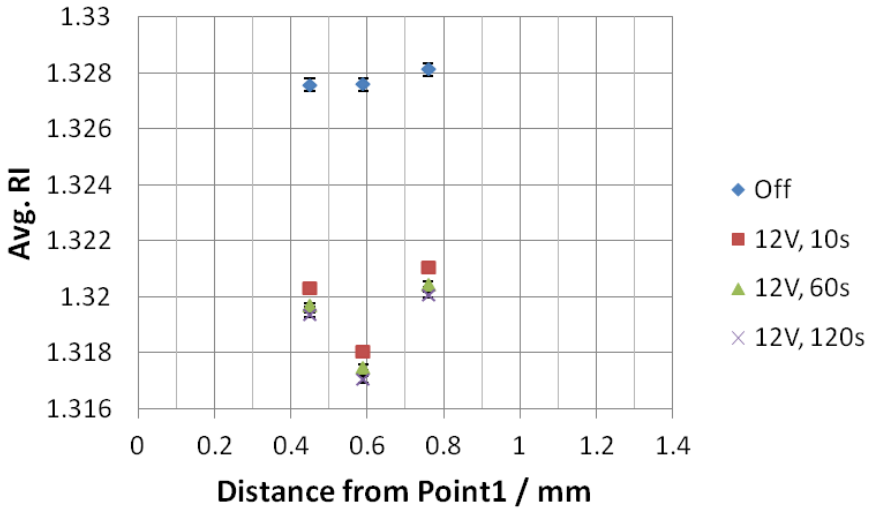

- A lateral refractive index distribution was measured.

Joule heating, Chip 05-Apr-2011

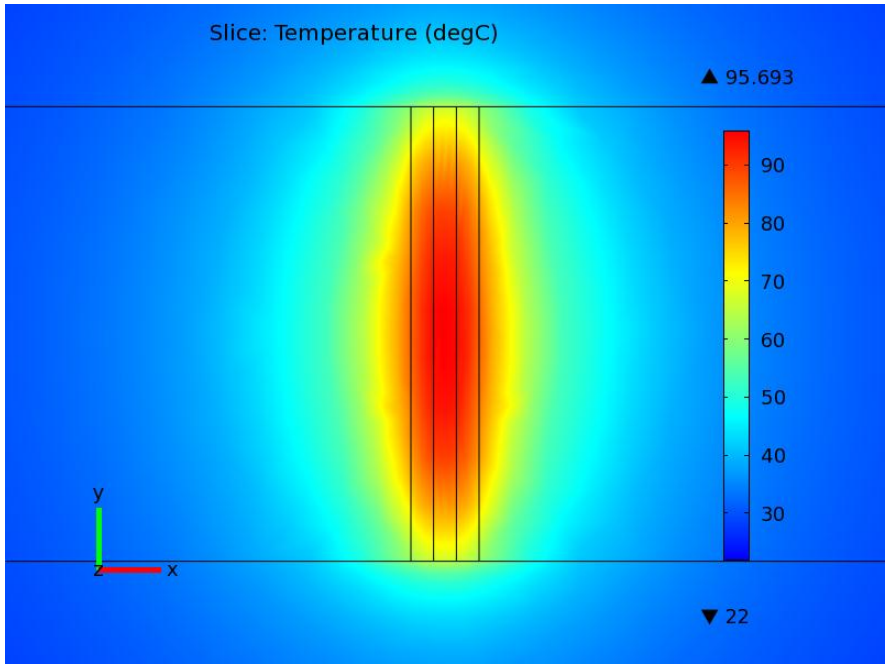

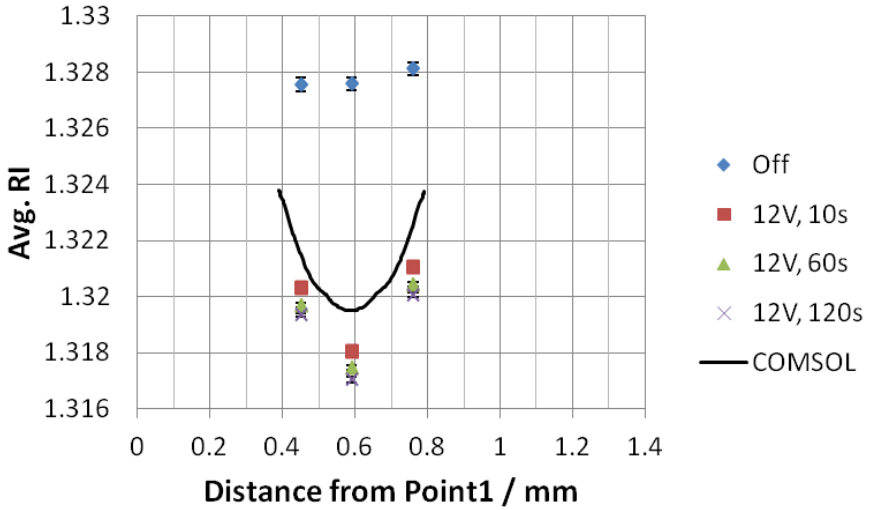

"Off" RI is 1.328 (=30°C) which is warm, could shift all data up by 10°C (=0.0016 RIU)

- COMSOL simulation utilized:
  - All temperature dependent parameters, where σ_0 = 1.25 S/m
  - Electrode width of 60μm
  - Channel height of 18.6μm
  - A voltage of 3.5Vrms, as approximately measured by the oscilloscope with 12V on the function generator
  - $n_{PBS}(T)$ from experimental work, $z=z_{avg}=5\mu m$, and a line at $x=+10\mu m$ away from electrode edge.

3) GRIN lenses

- The relative refractive indices are mapped (H–high, L–low)
- Light bends towards higher refractive indices.

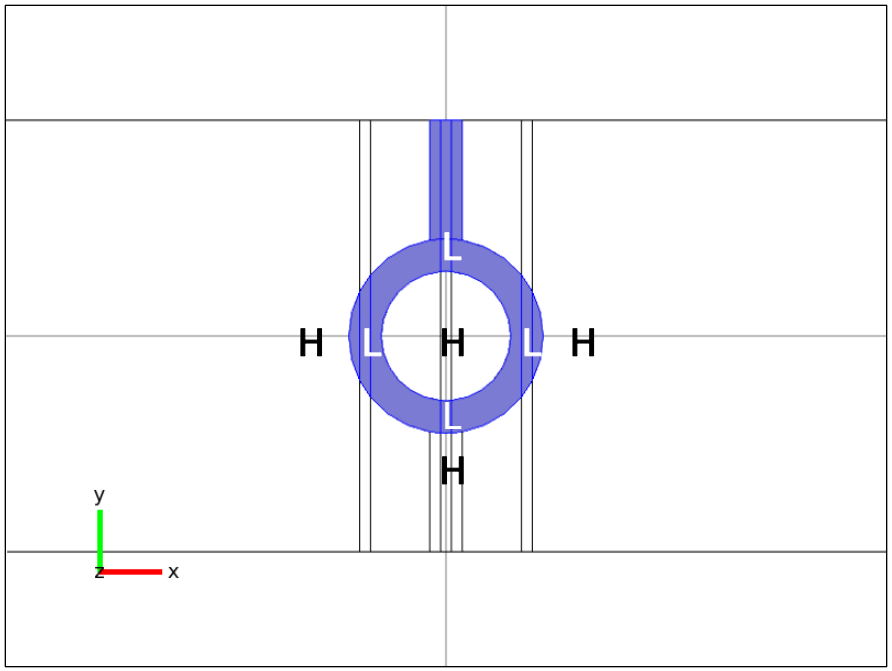

GRIN lenses

- Electrodes off

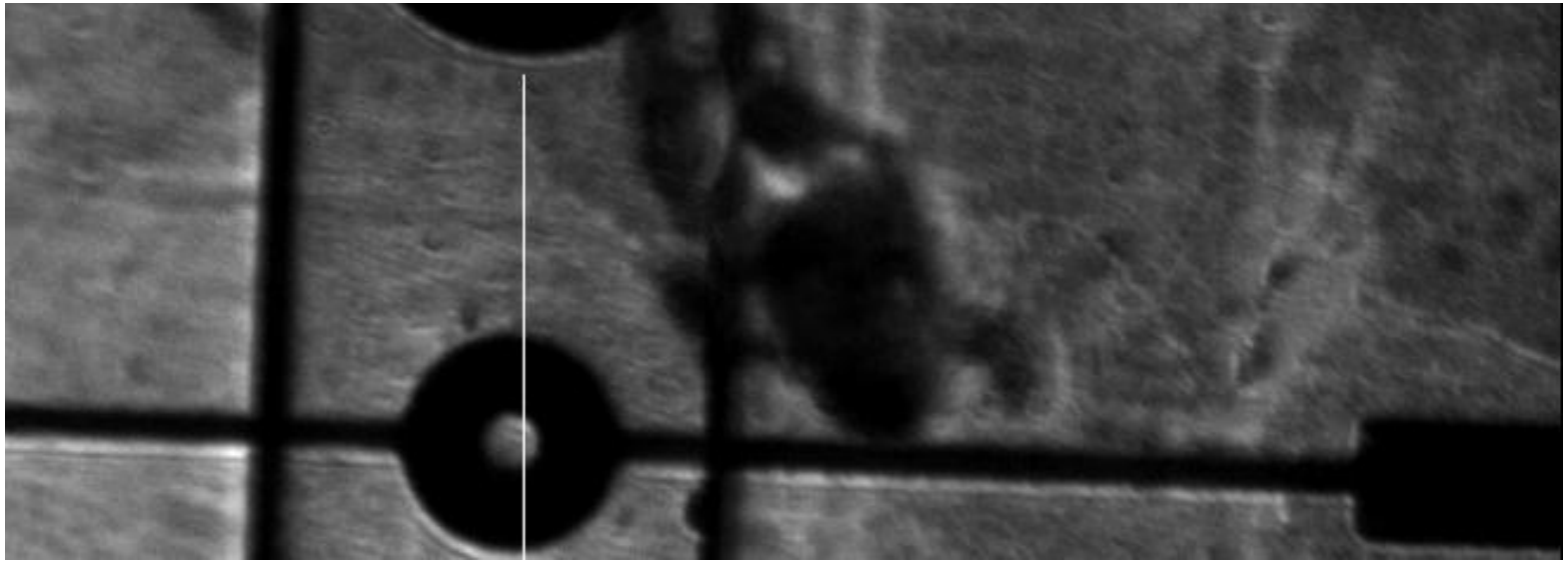

GRIN lenses

- Electrodes energized

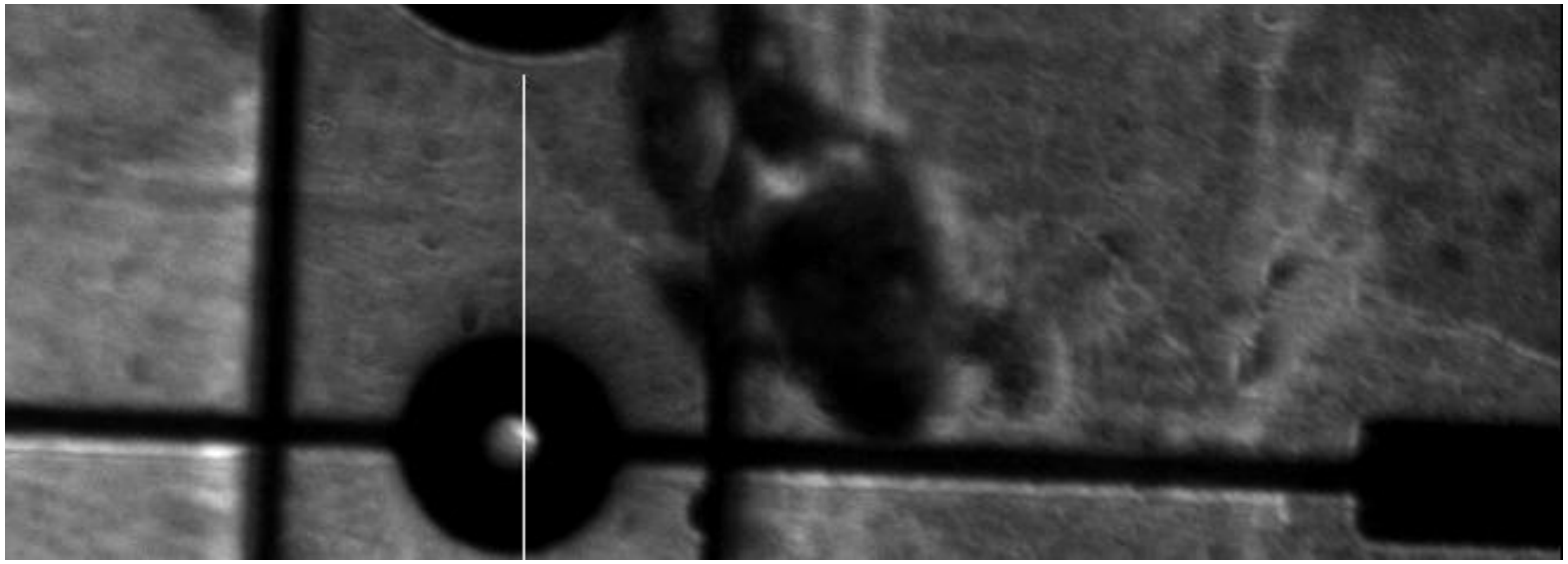

GRIN lens pixel intensity

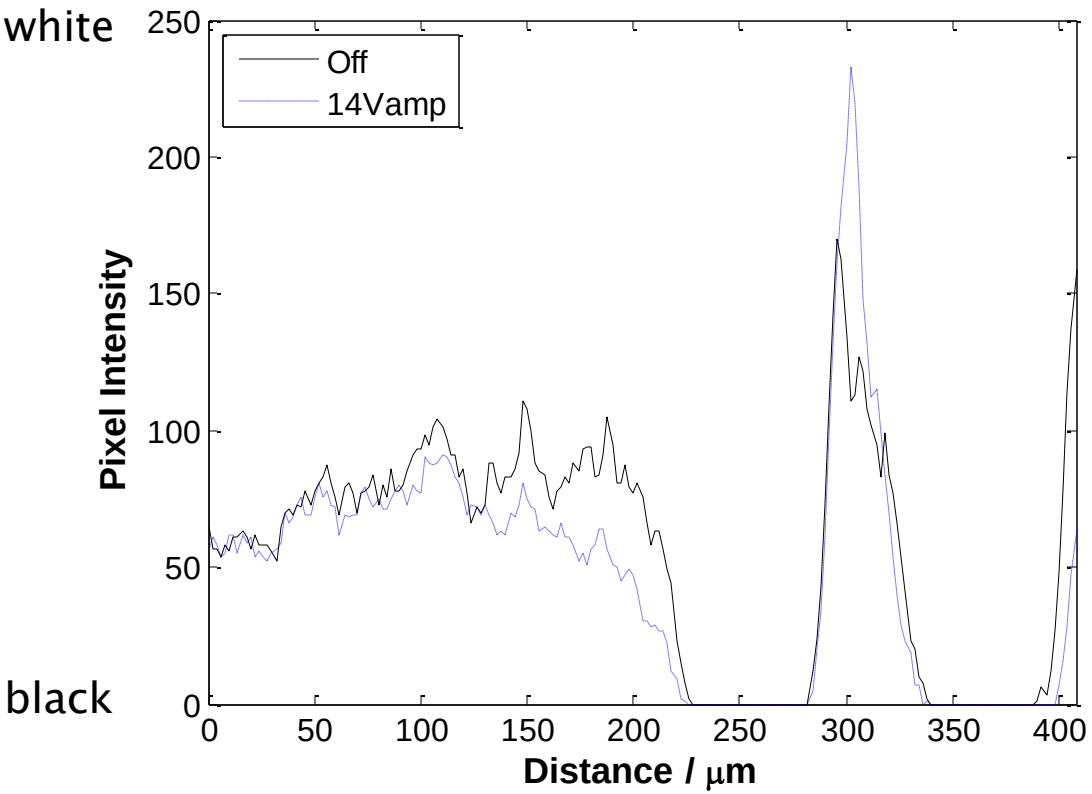

Summary

- A microfluidic refractometer was demonstrated with spatial, temperature, and wavelength dependence.
- Refractive indices were measured with sources of temperature from an isothermal apparatus as well as joule heating from energized electrodes. Problems were noted.
- Both positive and negative GRIN lenses were presented that result from temperature gradients from joule heating.
- Computer models were developed to compliment experimental work:
  - Electrostatic → electric field lines and magnitude, DEP force
  - Joule heating → temperature distribution, with improved physical accuracy using temperature dependent parameters
  - Optical → mirror penetration influence on FP transmission spectra
  - Optical → refractive index distribution (from joule heating), and predicted focal lengths from the parabolic parts of the RI

Journal and conference papers

- Journal papers:
  - R. Pownall, **J. Kindt**, and K. L. Lear, "AC Performance of Polysilicon Leaky-Mode MSM Photodetectors," *Journal of Lightwave Technology*, vol. 28, no. 18, pp. 2724-2729, 2010.

- Conference papers:
  - R. Pownall, G. Yuan, C. Thangaraj, **J. Kindt**, T. W. Chen, P. Nikkel, and K. L. Lear, "DC and AC performance of leaky-mode metal-semiconductor-metal polysilicon photodetectors," Proc. SPIE, vol. 7598, 2010. doi: 10.1117/12.843002
  - **J. Kindt**, M. Naqbi, T. Kiljan, W. Fuller, W. Wang, D. W. Kisker, and K. L. Lear, "Automated optical cell detection, sorting, and temperature measurements," Proc. SPIE, vol. 7902, 2011. doi: 10.1117/12.875608

Acknowledgements

- Dr. Buchanan and Dr. Notaros, committee members
- Dr. Lear, research advisor
- Dr. Kisker, outside advisor
- Optoe group members, including Weina Wang and Ishan Thakkar for chip fabrication

Thank you!

Additional slides

Cell viability with temperature

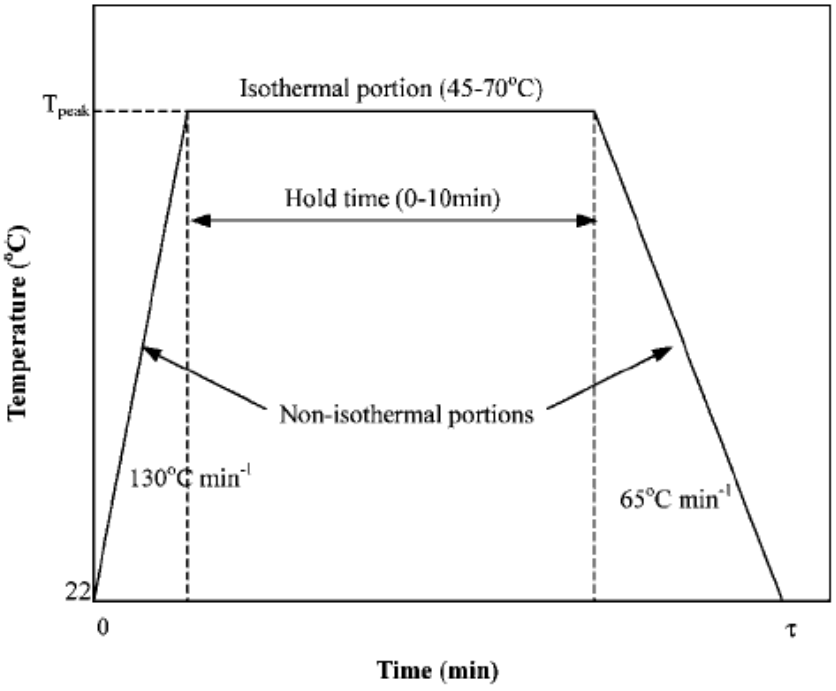

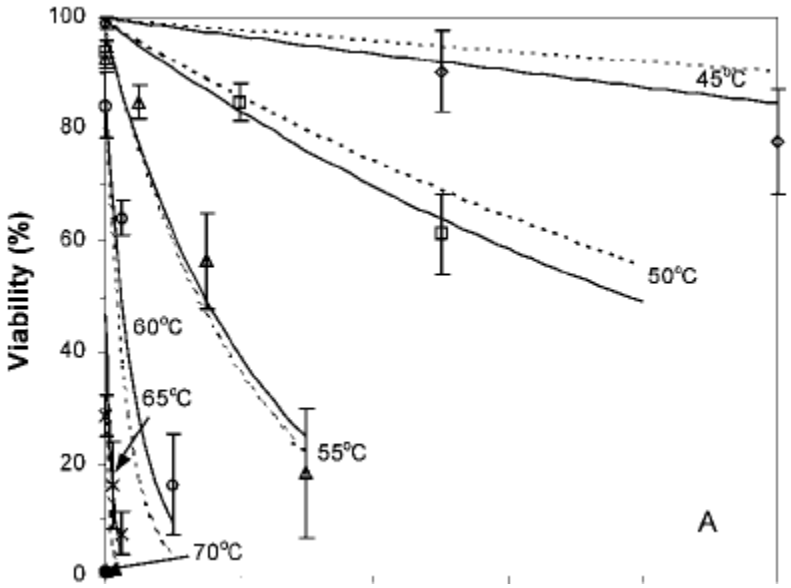

Measured and predicted cell viability vs. hold time at peak temperature for suspended SN12 cells. Therefore, subtract 22°C for temperature rise.

X. He and J. C. Bischof, *Annals of Biomedical Engineering,* vol. 33, no. 4, 2005.

Joule heating equation

- From COMSOL User's Guide:

$$\rho C_p \frac{\partial T}{\partial t} - \nabla \cdot (k \nabla T) = Q$$

- Where:
  - $Q = \sigma E^2$, upper limit of 40 GW m^{-3} ➔ 10 mW
  - Simulations are assumed steady-state

Electrostatic equations

From COMSOL's User Guide:

$$\mathbf{E} = -\nabla V$$

Gauss's Law:

$$\nabla \cdot \mathbf{D} = \rho$$

Where the constitutive relation is given by:

$$\mathbf{D} = \varepsilon_0 \mathbf{E} + \mathbf{P}$$

$$\mathbf{D} = \varepsilon_0 \mathbf{E} + \left(\varepsilon_0 \varepsilon_r \mathbf{E} - \varepsilon_0 \mathbf{E}\right) = \varepsilon_0 \varepsilon_r \mathbf{E}$$

$$\mathbf{D} = -\varepsilon_0 \varepsilon_r \nabla V$$

Therefore, Gauss's Law becomes:

$$-\nabla \cdot \left(\varepsilon_0 \varepsilon_r \nabla V\right) = \rho$$

$$-\varepsilon_0 \varepsilon_r \nabla^2 V = \rho$$

In a space-charge region:

$$-\varepsilon_0 \varepsilon_r \nabla^2 V = 0$$

$$\nabla^2 V = 0$$

Cavity stability with GRIN lenses

	Negative GRIN Lens	Positive GRIN Lens
Unit cell:	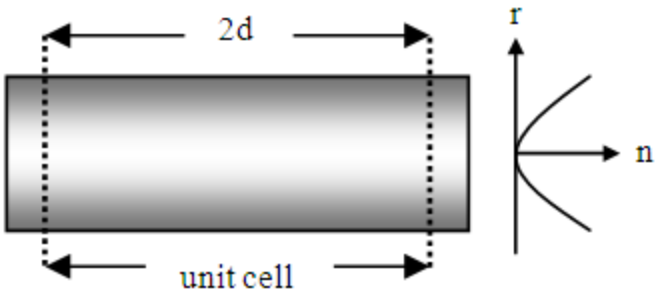	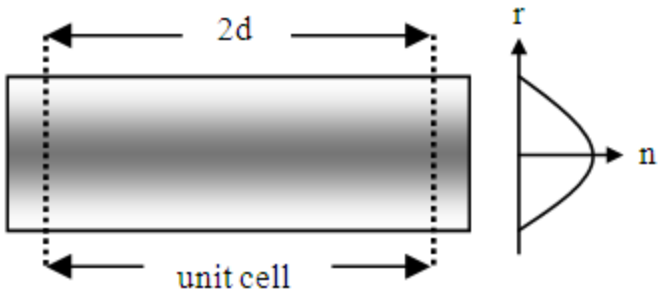
Unit cell matrix:	$\begin{bmatrix} \cosh\left(\frac{2d}{L}\right) & L\sinh\left(\frac{2d}{L}\right) \\ \frac{1}{L}\sinh\left(\frac{2d}{L}\right) & \cosh\left(\frac{2d}{L}\right) \end{bmatrix}$	$\begin{bmatrix} \cos\left(\frac{2d}{l}\right) & l\sin\left(\frac{2d}{l}\right) \\ -\frac{1}{l}\sin\left(\frac{2d}{l}\right) & \cos\left(\frac{2d}{l}\right) \end{bmatrix}$
Stability: $S = \frac{A+D+2}{4}$	$S = \frac{1}{2}\left\{\cosh\left(\frac{2d}{L}\right)+1\right\}$	$S = \frac{1}{2}\left\{\cos\left(\frac{2d}{l}\right)+1\right\}$
Stable when: $0 \le S \le 1$	Besides being conditionally stable when $L\to\infty$, cavity is not stable for any values of $2d/L$	Besides being conditionally stable when $l\to\infty$, or $2d/l = m\pi$, the cavity is stable

Focal length f = -1/C

Polymer swelling

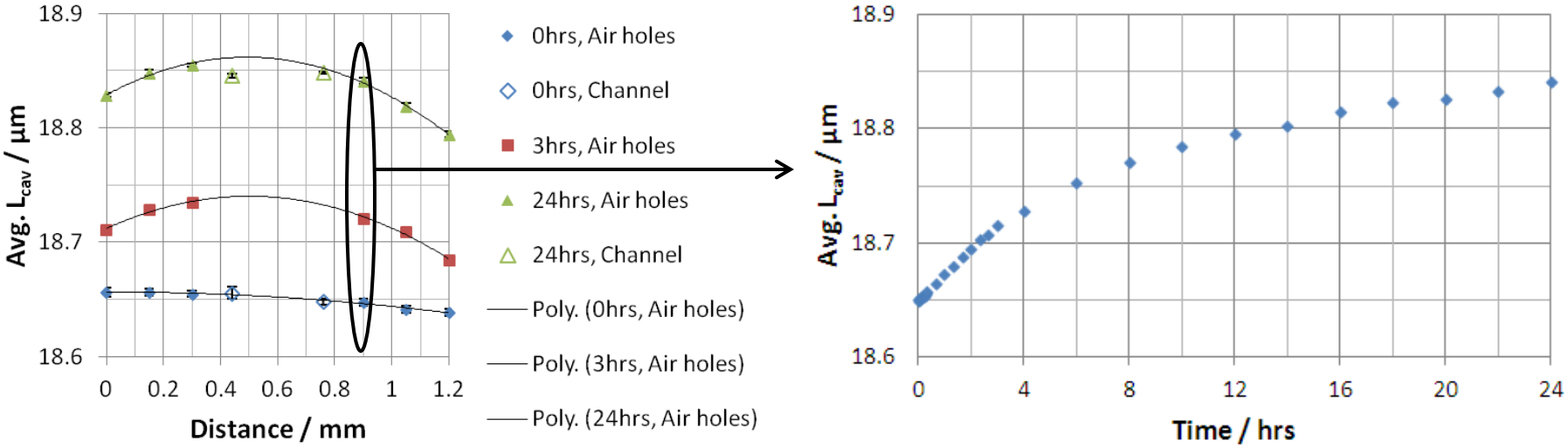

- It is better to use a total of 6 air holes:
  - A 2nd order polynomial does not fit very well for additional air holes due to the swelling profile.
  - Less air holes results in less measuring time. However, ~12 air holes were still measured (6 used) in the isothermal experiments.

- There are multiple occurrences of polymer swelling in the literature, including SU-8 and its baking dependence.

TFCalc references for H_2O, HfO_2, SiO_2

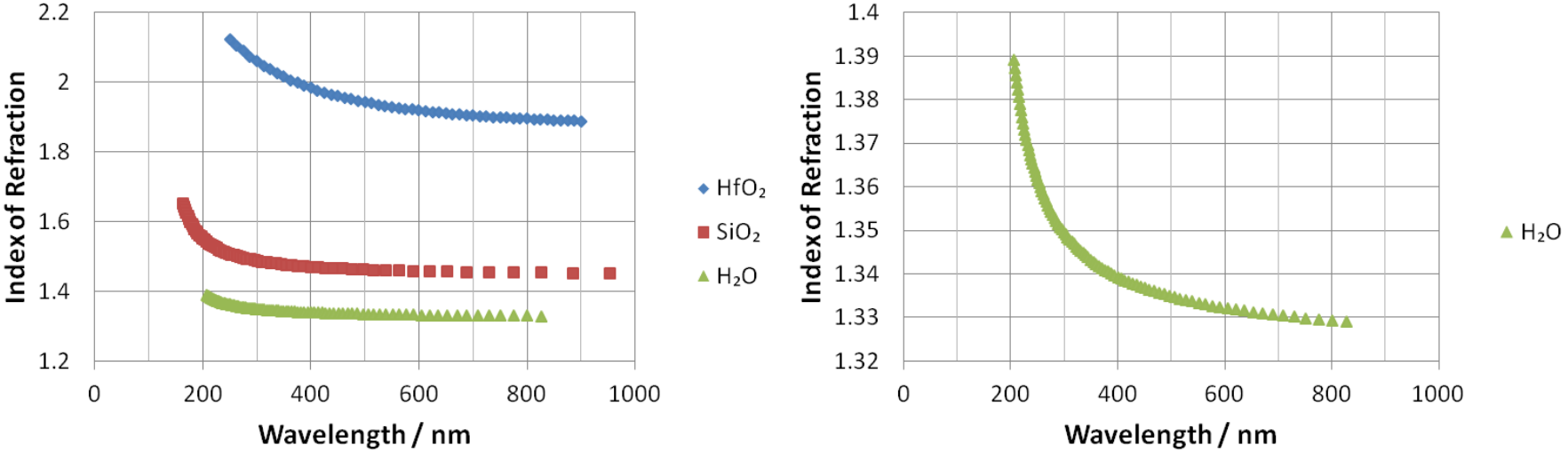

- From correspondence with TFCalc:
  - H_2O: Handbook of Optical Constants of Solids II, page 1059
  - HfO_2: Thin-Film Optical Filters, page 505
    Kruschwitz and Pawlewicvz 1997 OT Paper, page 2158
  - SiO_2: Handbook of Optical Constants of Solids, pages 719 and 749